UDC 004
21.3
681.5
In print: ISSN 2545 – 4250
On line: ISSN 2545 – 4269

JOURNAL OF ELECTRICAL ENGINEERING AND INFORMATION TECHNOLOGIES

СПИСАНИЕ ЗА ЕЛЕКТРОТЕХНИКА И ИНФОРМАЦИСКИ ТЕХНОЛОГИИ

J. Electr. Eng. Inf.. Technol.	Vol.	No.	pp.	Skopje
	9	2	75–115	2024
Спис. Електротехн. Инф. Технол.	Год.	Број	стр.	Скопје

J. Electr. Eng. Inf.. Technol.	Vol.	No.	pp.	Skopje
	9	2	75–115	2024
Спис. Електротехн. Инф. Технол.	Год.	Број	стр.	Скопје

JOURNAL OF ELECTRICAL ENGINEERING AND INFORMATION TECHNOLOGIES
СПИСАНИЕ ЗА ЕЛЕКТРОТЕХНИКА И ИНФОРМАЦИСКИ ТЕХНОЛОГИИ

Published by:
Faculty of Electrical Engineering and Information Technologies, "Ss. Cyril and Methodius" University in Skopje, P.O.Box 574, MK-1001 Skopje, North Macedonia

Издава:
Факултет за електротехника и информациски технологии, Универзитет „Св. Кирил и Методиј" во Скопје, пошт. фах 574, МК-1001 Скопје, Северна Македонија

Published twice yearly – Излегува два пати годишно

JOURNAL OF ELECTRICAL ENGINEERING AND INFORMATION TECHNOLOGIES
СПИСАНИЕ ЗА ЕЛЕКТРОТЕХНИКА И ИНФОРМАЦИСКИ ТЕХНОЛОГИИ

J. Electr. Eng. Inf.. Technol.	Vol.	No.	pp.	Skopje
	9	2	75–115	2024
Спис. Електротехн. Инф. Технол.	Год.	Број	стр.	Скопје

TABLE OF CONTENTS
(С О Д Р Ж И Н А)

Physics – Физика

Electrical Energy – Електроенергетика

Telecommunications – Телекомуникации

Journal of Electrical Engineering and Information Technologies, Vol. **9**, No. 2 pp. 79-86 (2024)
Article 221
Received: May 6, 2024
Accepted: November 5, 2024
In print: ISSN 2545–4250
On line: ISSN 2545–4269
UDC: 621.387.4:535.377]:546.33'131
doi.org/10.51466/JEEIT2492221079k

Original Scientific Paper

LUMINESCENCE PROPERTIES AND APPLICABILITY OF TABLE SALT AS AN ACCIDENT DOSIMETER IN RADIOLOGICAL EMERGENCIES

Aleksandar Krleski[1)] Ivana Sandeva[2)] Ralica Stanoeva[3)] Lihnida Stojanovska – Georgievska[4)] Hristina Spasevska[5)] Margarita Ginovska[6)]

[1,2,4,5,6]Ss. Cyril and Methodius University in Skopje, Faculty of Electrical Engineering and Information Technologies 1000 Skopje, Macedonia, [3]South Western University, Faculty of Mathematics and Natural Sciences, 2700, Blagoevgrad, Bulgaria

[1)] krleski@feit.ukim.edu.mk

Abstract: In the event of a nuclear incident, it is important to assess the population's exposure thereto at individual level. In retrospective dosimetry, the absorbed dose is determined from materials that have wide application in everyday life. In the early stages after the accident, results obtained with retrospective dosimetry methods are used for triage and allow actions taken to focus on places where they are most needed, that is, they serve as support for making strategic decisions of action. Dosimetric data, in addition to assessment of individual doses, can also be used to assess long-term effects, as well as to improve epidemiological analyses. Materials suitable for examination with luminescent techniques are electronic components, building materials from which quartz can be isolated, porcelain, or dental ceramics.

Crystals characterized by good response to optically or thermally stimulated luminescence and widely distributed in the environment are very useful in retrospective dosimetry for dose estimates in nuclear incidents. When exposed to ionizing radiation, common salt, mainly comprised of NaCl, is a material that exhibits significantly greater luminescence than many other materials. The aim of this study is to investigate thermoluminescence (TL) and optically stimulated luminescence (OSL) characteristics of commercially available table salt.

A protocol for measuring luminescent properties in materials for retrospective dosimetry was applied. Both irradiated and non-irradiated samples showed satisfactory TL/OSL responses. A linear dose response was observed, identifying the material as suitable for retrospective dosimetry. Preheating and reading temperatures were determined, and the SAR method yielded highly accurate dose measurements.

Keywords: retrospective dosimetry, thermoluminescence, optically stimulated luminescence

ЛУМИНИСЦЕНТНИТЕ СВОЈСТВА И ПРИМЕНЛИВОСТ НА ГОТВАРСКА СОЛ (NACL) ЗА РЕТРОСПЕКТИВНА ДОЗИМЕТРИЈА

Апстракт: Во случај на нуклеарен инцидент, важно е да се направи проценка на изложеноста на населението на индивидуално ниво. Во ретроспективната дозиметрија, апсорбираната доза се одредува од материјали кои имаат широка примена во секојдневниот живот. Во раните фази по несреќата, резултатите добиени со ретроспективни дозиметриски методи се користат за тријажа и овозможуваат преземените постапки да се фокусираат на местата каде што им се најпотребни, односно служат како поддршка за носење стратешки одлуки на дејствување. Дозиметриските податоци, покрај проценката на индивидуалните дози, може да се користат и за проценка на долгорочни ефекти, како и за подобрување на епидемиолошките анализи. Материјали кои се погодни за испитување со луминисцентни техники се електронски компоненти, градежен материјал од кој може да се изолира кварц, порцелан, стоматолошка керамика, итн.

Кристалите кои имаат добар одговор на оптички стимулирана луминисценција или термолуминисценција и се широко распространети во околината во која живееме се многу корисни во ретроспективната дозиметрија за проценка на доза при нуклеарни инциденти. Готварската сол, која главно се состои од NaCl, е материјал што покажува значително поголема луминисценција од повеќето други материјали кога се изложени на јонизирачко зрачење. Целта на ова истражување е да се испитаат карактеристиките добиени при термолуминисценција (ТЛ) и оптички стимулирана луминисценција (ОСЛ) на комерцијално достапна готварска сол.

Применет е протокол за карактеризација на луминисцентните својства во материјалите погодни за ретроспективна дозиметрија. Од испитувањето на озрачените и неозрачените примероци се покажа задоволителни TL/OSL одговори. Од испитувањето забележан е линеарен одговор на дозата, идентификувајќи го материјалот како погоден за ретроспективна дозиметрија. Беа утврдени температурите за предзагревање и читање, а методот SAR даде многу прецизни мерења на дозата.

Клучни зборови: ретроспективна дозиметрија, термолуминисценција, оптички стимулирана луминисценција.

I. INTRODUCTION

DOSE reconstruction can include various physical and biological measurement methods as well as numerical analyses of radioactivity data records. Dose reconstruction based on dose measurements performed on individuals includes methods that estimate the absorbed dose by examining teeth, blood, and radionuclide activity in the body. For external exposure, the appropriate methods are usually based on persistent effects, such as free radicals or electrons trapped in defects (imperfections in crystal structure) in minerals, products of neutron activation, or changes in blood constituents. Measurements of radionuclides in the human body can be used for internal exposure.

Luminescent dose reconstruction methods are particularly suitable for determining doses to population groups caused by external exposure to gamma radiation. For individuals or population groups, additional modeling is required to transform the absorbed dose measured by luminescence methods.

Use of ionizing radiation, even in tightly controlled conditions, for example, in medical diagnostics or radiotherapy, is associated with certain risk of error and delivery of unwanted dose to the patient or personnel operating the equipment. In such cases, the delivered dose for patients and portion of support staff not covered by dosimetric monitoring can only be determined by retrospective dosimetric methods. Moreover, the threat of nuclear weapons use becomes a potential risk in the 21st century. The degree of risk of another nuclear power plant accident still exists, and with it, also the risk of mass radiation exposure. Even countries that nowadays use ionizing radiation only for peaceful purposes face the risk of mass contamination, in which case they would have to be prepared for rapid and accurate assessment of the dose received by the population in the event of a mass nuclear incident.

This paper focuses on characterization of widespread table salt, as well as nutritionally enriched salts that are increasingly used (magnesium chloride, potassium chloride, etc.).

In the last decade, different household salts have been subject of numerous optically stimulated luminescence (OSL) and thermoluminescence (TL) studies in respect to retrospective dosimetry purposes. Sea and rock salts are very well established as highly sensible material for (OSL) dosimetry. Existence of pre-established repository of well characterized materials, as fortuitus dosimeters, as well as a set of characterized instruments that collectively form a dosimetric system, assumes significant importance in facilitating prompt responsiveness during a nuclear incident. Thus far, extensive research efforts have been dedicated to investigating potential utilization of salt as retrospective dosimeter. Substantial variations in luminescent properties are observed, depending on the type of salt and its geographical origin. In almost all cases, examination of luminescent properties of salts by optically stimulated luminescence is accompanied by thermal processes of preheating or readout with heating.

Bailey et al. investigated OSL properties in respect to its applicability in dating and dosimetry of NaCl relative to dating and dosimetry of commercially obtained analytical quality NaCl, using a Risø TL DA-12 reader with blue, green, and IR continuous wave stimulation (CWS) light. They obtained linearity of OSL signal for doses up to 10 Gy. In their protocol, the salt is preheated to 200°C and read at 120°C [1]. Other research done by Go Okada et al. investigated OSL properties of Eu2+ doped NaCl single crystal using a lab-constructed automated system with CWS 450-550 nm. During the preparation process, the powder was dehydrated by heating at 500°C overnight. The sample was irradiated with X-rays. They obtained linearity of OSL signal for doses up to 10 Gy [2]. TL properties were researched by Datz et al. on 10 brands of Israeli household salt (NaCl) using a Thermo 3500 manual reader with an IR filter. Readout temperature was between 50 and 350˚C at a linear heating rate of 1 and 5˚C s^{-1}. The samples, weighing 50 mg on average, were irradiated using a calibrated gamma-ray ^{137}Cs source with a dose ranging from 0.5 mGy to 300 Gy. Eight of the ten brands showed similar glow curves. They concluded that the salt with a higher dopant concentration is significantly more sensitive [3]. Alghamdi et al. have demonstrated that dosimetry using common salt with portable OSL reader is a rapid and effective means of determining dose below 100 μGy. For the purpose of dose response, experiments were made with photon irradiation in the range 20–500 μGy. Detection limits of 7 μGy have been successfully demonstrated for OSL measurements, while the other instruments examined had shown detection limits ranging from 30 to 340 μGy. The most sensitive systems were able to determine dose responses within the range of 0 to 500 μGy. These systems exhibited a linear response across this dose range, with a non-zero intercept indicating doses received from environmental sources since the salt's production. Measurements of salt samples that had been exposed to artificial daylight for 1 week showed luminescence signals significantly above the empty chamber, especially with 890 and 470 nm stimulation [4]. Majgier et al. investigated OSL properties of potassium chloride and its potential use in radiation dosimetry. In addition, these properties were compared to that of NaCl in the same type of physical forms. KCl was studied in three sample forms: powder, crystal and pellets, using a Risø TL/OSL-DA-15 reader with blue continuous wave simulation light with peek emission at 470 nm. Irradiations inside the TL/OSL reader were carried out using beta source with a dose rate of ~0.80mGy s^{-1}. All KCL samples (powder 60% 500–700 μm, crystal grains with grain sizes from 2 to 5 mm, and pellets 5mm diameter × 1mm thickness, ~50 mg mass) were irradiated with an absorbed calibration dose (CD) of 0.44 Gy, stored for 150 s, and then OSL signal was read out at various temperatures from 25°C to 300°C. Heating to the set readout temperature was performed using a heating rate of 5°C/s. After that, a test dose of 0.044 Gy was administered and the corresponding OSL signal was acquired. For NaCl powder, readout settings were the following: preheating at 220°C

and a 40 s OSL readout at 100°C with 40% of maximal continue wave blue LED stimulation power. Additional measurements were also made at room temperature and without preheat [5]. Janet Ayobami Ademola has shown that, within the limit of error, salt samples could be used as complementary emergency dosimeter in radiological accident situation (OSL and TL luminescence). Two samples were dried at room temperature and placed on plantchet sprayed lightly with silicon. The samples were irradiated with beta-irradiator (618 mGy) holding a calibrated $^{90}Sr/^{90}Y$ source. For irradiated samples (with heating rate of 5℃/s), TL peaks occurred at about 100℃, 240℃ and 280℃. OSL signals of irradiated samples (410 mGy) started to decay at about 0.49 s and decayed to negligible proportion after about 5 s. Two samples were used to test for fading, irradiated with 1000 mGy beta dose and stored in dark, at room temperature, for a period of 0 - 14 days. OSL measurements were done at stimulation temperature of 125℃ for 40 s, with a heating rate of 5℃/s. The samples were preheated to temperature of 190℃ at 5/s for 10 s before OSL measurements. The two samples exhibited little fading over 14 days, with more than 80% of the signal remaining [6].

Katarzyna et al. demonstrated OSL dosimetric properties of dietary supplements containing potassium chloride (KCl). CW-OSL measurements were performed using a Helios OSL reader with green continuous wave simulation light. Equal samples weighing 100 ± 3 mg with similar surface area were prepared and irradiated with a dose of 2.5 Gy before reading CW-OSL signal. Dose response characteristics were observed in a range from 0.05 Gy to 11.65 Gy immediately after irradiation and 24 h after irradiation. The dose recovery test was performed for doses: 0.61 Gy, 1.84 Gy and 3.07 Gy, representing the radiation dose triage levels. Linearity in the dose response was present in two ranges: 0.05-0.9 Gy and 0.9 to 9.5 Gy [7].

Bernhardsson et al. have investigated the potential of a selection of household salt as retrospective dosemeter for ionizing radiation using optically stimulated luminescence (OSL). The salt was carefully mixed in a dark room and was irradiated at distances of 5.5 and 0.5 m, with dose rates of 21 $\mu Gy\ s^{-1}$ and 2 $mGy\ s^{-1}$. Following the irradiation, the salt was kept inside light-sealed tubes for 24 h before readout. A linear dose response relationship was found in the dose range from 1 mGy to about 100 mGy, while above that level, the relationship becomes moderately supra-linear, at least up to 9 Gy. The two sea salts and the dissolved mine salt showed dominating glow peak at around 100°C [8].

Fujita et al. investigated optically stimulated luminescence (OSL) and violet thermoluminescence (VTL) characteristics of "Aji-Shio" (Ajinomoto), Japanese commercial salt. An automated Risø TL/OSL DA15-B reader was used in all OSL and violet TL (VTL) measurements, using blue continuous simulation lights with maximum emission at 470 ± 30 nm. The SAR (single-aliquot regenerative-dose) protocol (using blue-LED simulation) was established. The samples were first irradiated with a dose of 2 Gy and then preheated to 160˚C for 10 s. OSL measurements were then carried out at 60˚C for 40 s. A test dose of 0.5 Gy was then given, followed by second preheating done at 100˚C for 30 s. OSL simulation was done again at 60˚C for 40 s, and afterwards the samples were illuminated for 40 s at 160˚C [9]. Fuochi et al. studied Gamma-irradiated NaCl samples of different origin using PSL technique. Irradiation was performed with ^{60}Co gamma rays. The dose rate at the sample location was 0.6 Gy/min, with an uncertainty in dose delivery of about 2% at 1 SD. The number of photon counts recorded in 60 s was taken as PSL measurement result. PSL response increases linearly with sample mass up to about 10 g and saturates at about 20 – 25 g. High PSL positive results of rock salt suggest that the material has stored the natural radiation background on a geological time scale. This information was lost during the industrial preparation process of refined table rock salt which led to negative PSL classification. To reset the geological PSL signal to zero, all salt samples were annealed at 150℃ for 1 h before irradiation. The irradiation doses were limited to 0.5 and 1 Gy, since the very high geological signal of rock salt suggested its high sensitivity. Dose response behavior of sea salt and refined rock salt was studied in the 0.1 – 2 Gy range. Doses were limited to 2 Gy to avoid counter overflow. Measurements were performed 24 h after irradiation. Even the samples kept in dark under normal laboratory conditions showed a fast decay within the first few days. After 20 days of storage, PSL readings decreased to about 20% of the initial values. TL measurements were made on about 30 mg aliquots in the range 70℃ – 380℃, with a heating rate of 6℃/s. The glow curve of rock salt presents a peak in the high temperature region, typical of geological signals [10].

Lopez et al. investigated CW-OSL dosimetric properties of natural NaCl samples, collected in the Dead Sea, using a custom-made OSL equipment with blue continuous simulation light, with maximum emission at 455 ± 25 nm. Luminescence of the stimulated sample was observed trough two U 340 filters. CW-OSL dose response was analyzed from 0.2 up to 20 Gy of ^{60}Co gamma radiation. Natural NaCl minerals showed a linear CW-OSL dose response range between 0.5 and 10 Gy, obtained at room temperature (~25 ˚C). The samples exhibited an enhancement of sensitivity when preheated between 130˚C and 190˚C, as well as an increase of CW-OSL response when stored in a time period of 336 h [11]. Spooner et al. studied NaCl samples, analyzing its high sensitivity to ionizing radiation, by thermoluminescence (TL), optically-stimulated luminescence (OSL) and infrared-stimulated luminescence (IRSL). 8 mg of sample grains were loaded onto stainless discs and preheated at 2K/s to each of 8 different temperatures spaced in 10℃ increments from 190℃ to 260℃ and irradiated with 0.13 Gy $^{90}Sr/^{90}Y$ beta radiation. Preheating to 300℃ and higher temperatures created a significant new 100℃ TL peak in the UV (370 nm) emission band while desensitizing the 590 nm TL emission. The Pulse anneal analysis of OSL and IRSL was done in two stages. Firstly, the samples were irradiated with 0.26Gy, and OSL was measured using 12s exposure. Secondly, measurements were made to reveal thermal draining of the traps by increasingly high temperature

preheating. 0.26 Gy dose was administered to each disc, the first illumination was done at 30℃ for 0.2 s. Temperature was incremented in 20℃ steps until 140℃, then in 10℃ steps to 300℃, between each the sample was returned to 30℃ and monitor exposure was being made. OSL showed a slight increase in sensitivity as the annealing temperature approached 100℃, then dropped at a rate paralleling thermal erosion of 100℃ TL peak. There is no significant source of OSL or IRSL (room temperature readout) that survives heating to temperatures beyond about 240℃. TL, OSL and IRSL sensitivity changes, confirmed activation of sensitivity change by exposure to temperatures exceeding 160℃ [12].

Spooner et al. studied TL, OSL and IRSL (infrared-stimulated luminescence) properties of 19 NaCl samples and their potential use in retrospective dosimetry. Sample characterization was done using the University of Adelaide Fourier-Transform thermoluminescence spectrometer to measure natural TL (NTL) and artificially-dosed TL (ATL) emissions. Kinetic analysis was done on each sample, whose sizes varied between 180-250μm grains, with a modified Alldred glow oven using an EMI 9635QA PMT colour glass filter. OSL, IRSL and TL dose response curves for UV and blue-to-orange emissions were constructed following beta irradiation (90Sr/90Y) for doses of 0, 0.14, 0.27, 0.54, 1.1, 2.2, 4.4, 8.7, 17.5 and 35 Gy. These experiments were performed using a Risø TL/OSL DA-20 reader with an EMI 9235QB PMT filter, with a heating rate at 2K/s in flowing nitrogen. Luminescence sensitivity of 590nm TL and blue-stimulated UV OSL was sufficient to enable dose detection limits of < 1mGy to be readily achievable for reported samples [13]. Tanır et al. studied infrared stimulated luminescence (IRSL) decay from NaCl using only one aliquot irradiated with a range of 2Gy to 200Gy β-radiation doses. The dose rate given to samples was 0.034Gy/s. The bleaching is carried out by exposing to daylight (or LED) and controlled by measuring signals from the sample. A single aliquot prepared from NaCl sample was given the β-radiation dose, preheated at 200 C for 1 min/IRSL was measured/it was bleached. These procedures were repeated for 2, 4, 6, 10, 15, 20, 30, 50, 75, 100 and 200 Gy doses for the same aliquot. Continuous decrease at low doses (2, 4 and 6 Gy) and an initial increase in intensity at high radiation doses (10 Gy) was observed. IRSL from NaCl has shown that the initial dose dependence at low doses is linear, followed by an approach to saturation at high doses. IRSL dose response from NaCl was saturated at ~ 50Gy. IRSL signal of NaCl has been shown to be decayed as being dose-dependent [14].

To carry out these investigations, it is first necessary to establish a protocol for luminescent reading of various materials, as well as to determine the linear region of the luminescent response suitable for use in dosimetry, and to apply the established protocol. In addition, the characteristics of investigated materials are provided by using deconvolution methods. Deconvoluted thermoluminescent curves determined some characteristics of the crystal structure of investigated materials. An assessment of measurement uncertainty for the reconstructed dose was also made.

II. Theoretical Background

Electrons of a single atom are allowed to exist in certain discrete energy levels. When a number of atoms form a solid, bands of allowed energy states are formed, separated by forbidden energy bands.

When defects (imperfections) are present in the crystal structure of a solid, electrons can move between valence and conduction band, leaving free electrons in the conduction band and free holes in the valence band. By this, new localized energy levels in the band gap are formed. When minerals are exposed to ionizing radiation, electrons may gain enough energy to leave their energy band and remain trapped in some imperfections of the crystal lattice. When this material is later exposed to optical or thermal stimulation, trapped electrons may gain enough energy to release and recombine with holes. The result of such re-combinations is emission of photons.

Thermoluminescence is the phenomenon of emission of light from irradiated solids when exposed to thermal stimulation, while optically stimulated luminescence is the phenomenon of emission of light from irradiated solids when stimulated with light of certain wavelengths. When TL- or OSL-sensitive material is exposed to ionizing radiation, electron-hole pairs are formed and move freely through the conductance and valence band. Some of them may be trapped in some active points. Electrons remain in this state until they gain enough energy from the stimulation to be released, after which they recombine with holes.

Luminescence signal is detected by photon counting method.

III. Materials and Methods

This study analyzes table salt found on the open Macedonian market. The declared composition of the examined salt is 99.9% table salt, potassium iodate and E 535 (sodium ferrocyanide). The examined salt sample contains KIO_3, in the amount of 20 to 30 mg of iodine per 1kg of salt.

Measurements are performed with the Riso TL/OSL reader, model DA-20, at the Radiation Physics Laboratory (RAD-LAB) within the Faculty of Electrical Engineering and Information Technologies in Skopje.

The apparatus is comprised of sample carousel and sensitive photomultiplier. The sample is placed on heater plate and then heated by thermocouple. Emitted light is focused towards the photomultiplier through a filter. Main parts of the TL/OSL reader used are sample chamber with sample holder that holds samples for measurement in certain position, heating system that controls sample temperature, light stimulation system that provides light sources for OSL, photomultiplier tube that detects emitted luminescence, filter system which filters out unwanted wavelengths, and control/data acquisition system software that manages operations and data.

A schematic diagram of the instrument is shown in Figure 1.

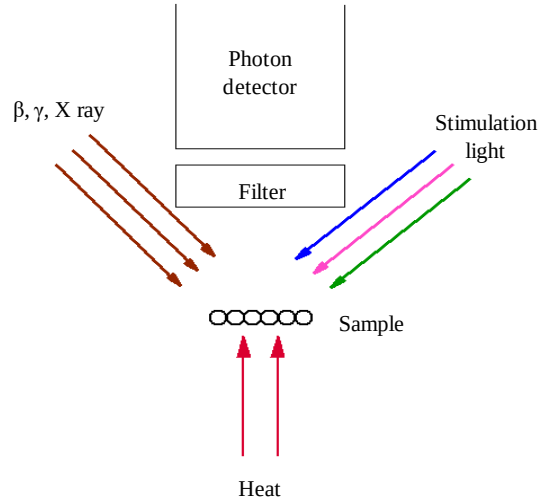

Fig. 1. Schematic diagram of the Riso TL/OSL reader

By using filters, the sample may be stimulated with light of different wavelengths. Intensity of the stimulating light is approximately 1018 times higher than the intensity of the light emitted from the sample. 90Sr beta source is used as source of radiation, embedded in the instrument. The beta source is characterized by activity of 1.48GBq (~0.1 Gy/s) and maximum energy of 2.27MeV. The beta dose actually comes from the decay of 90Sr, i.e., 90Y.

Figure 2 shows the protocol for determining luminescent characteristics regarding the material's application in retrospective dosimetry.

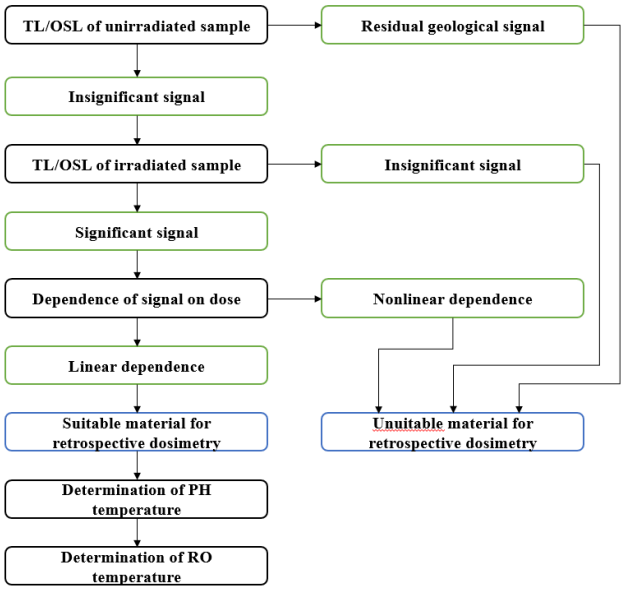

Fig. 2. Protocol for determining luminescent characteristics for the material's application in retrospective dosimetry

The protocol connects measurement procedures - marked with black outline, interpretation of the results obtained from measurement procedures - marked with green outline, and conclusions about the material's acceptability as retrospective dosimeter - marked with blue outline. Measurement procedures and interpretations are explained in detail below.

A. Deconvolution

For deconvolution of TL glow curves of irradiated samples, the software TL/OSL glow curve analyzer was used. By analyzing glow curves, some kinetic parameters of the samples could be calculated. New software for automatic glow curve deconvolution was used. The program provides values of kinetic parameters, glow peak area, and FOM as summing discrete (FOK, GOK) or continuous distribution of traps [15].

B. Results

Measurements were made for table salt samples from the open Macedonian market.

Beta source in the Riso TL/OSL reader is calibrated by sensitized quartz grains with dimensions in the interval 180-250μm, irradiated with 137Cs source with a dose of 4.81Gy from the Nordic Center for Luminescence Research. From the calibration curve obtained, it was calculated that the source's dose rate is 0.085Gy/s.

Measurements with TL and OSL were made on non-irradiated table salt sample and irradiated sample, with a dose of 300 mGy.

TL glow curves of non-irradiated, irradiated, and irradiated sample after illumination are shown in Figure 3. TL testing was performed with temperatures up to 400°C, with a heating rate of 5°C/s using U-340 optical filter. Measurements were conducted on non-irradiated salt sample, and two different irradiated salt samples: one exposed to a dose of 300 mGy and the other exposed to the same dose, but subjected to blue light illumination prior to TL measurement. TL signal emitted by the non-irradiated salt sample proved to be negligible, indicating absence of residual geological signals, making the salt suitable for retrospective dosimetry applications. Analysis of TL glow curve revealed three prominent peaks occurring at approximately 90°C, 200°C, and 220°C (Fig.2 for irradiated sample). Notably, the third peak is attributed to light-insensitive loop, as evidenced by the persistence of discernible TL signal even after illumination.

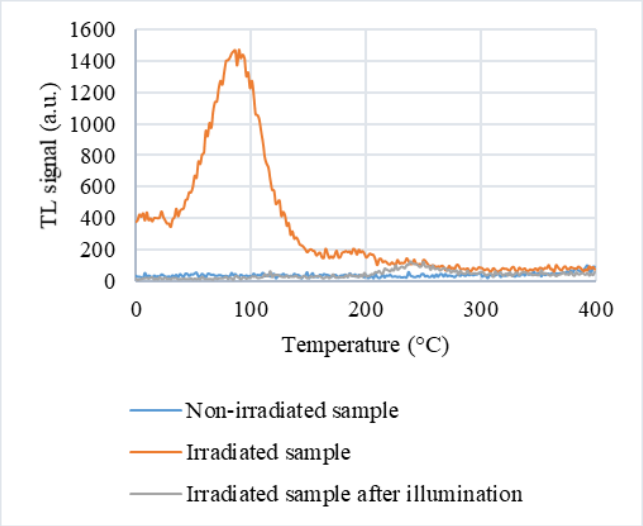

Fig. 3. TL signals of non-irradiated, irradiated sample (300 mGy), and irradiated sample (300 mGy) after illumination

Emission of OSL signal is presented in Figure 4. OSL measurement was performed with blue light at 60% power, without preheating. Measurements were conducted on non-irradiated salt sample and irradiated salt sample exposed to

a dose of 300 mGy. OSL signal emitted by the non-irradiated salt sample proved to be negligible as in TL investigation. OSL signal of irradiated sample dropped to an insignificant level already after two seconds of illumination.

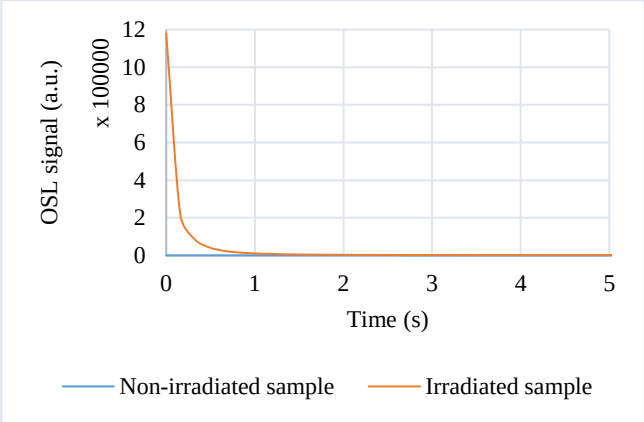

Fig. 4. OSL signals of non-irradiated sample and irradiated sample (300 mGy)

Dependence of the luminescent response is an important condition for the investigated material to be used as dosimeter. The luminescent signal response was measured by TL and OSL at doses from 100 mGy to 2600 mGy (Fig.5). The integral of the glow curve from 60°C to 300°C is considered as response for TL measurements, while for OSL measurements, an integral up to 1.5 s is taken as response.

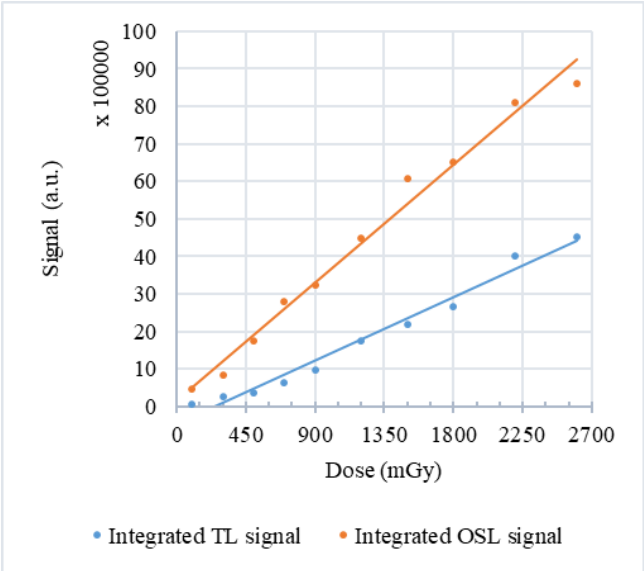

Fig. 5. Dependence of the luminescence signal on the dose

Comparison of preheating temperature TPh dependence of OSL response with TL glow curve is shown in Figure 6. Optimal preheating temperature is determined from the results. Stability of OSL signal is examined depending on the preheating temperature. The following test sequences were used:

1. Irradiation of each sample with a dose of 300 mGy;
2. Preheating at TPhi °C (heating rate 5°C/s) for 10 s;
3. OSL stimulation at 125°C (heating rate 5 °C/s) for 40 s;
4. Repeating sequences (1) to (3) from TPh1 = 60°C with increasing preheat temperature TPhi by 20°C.

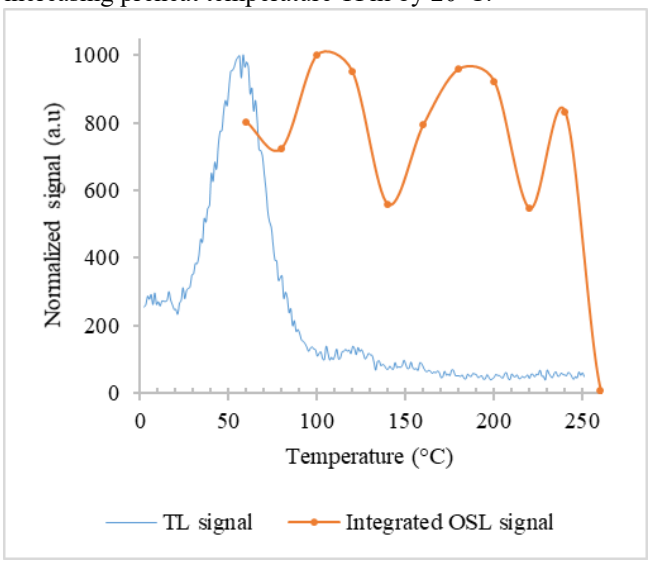

Fig. 6. Comparison of preheating temperature dependence of OSL response with TL glow curve

Each measurement was performed with a new aliquot of the same mass to eliminate the change in sensitivity due to heating.

The results obtained show two local minima of the integrated OSL signal with a value of about 600 normalized units at 140°C and 220°C. The value 140°C was chosen for preheating temperature.

In order to determine the optimal readout temperature T_{Ro}, an examination of OSL signal's dependence on the readout temperature was made (Fig.7.).

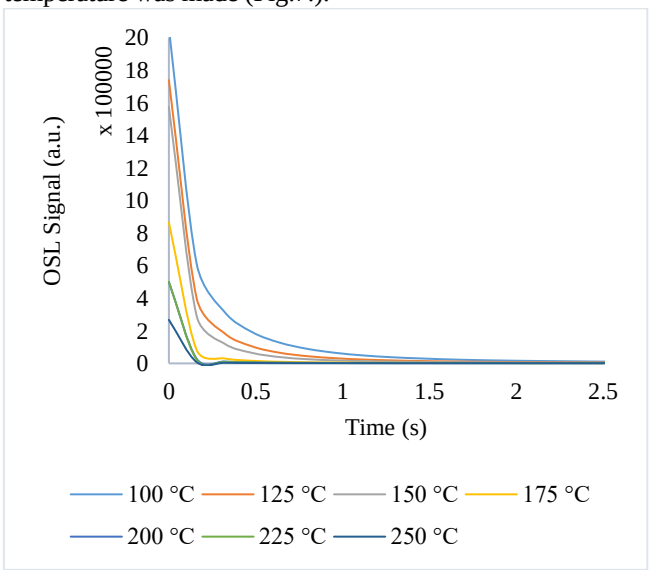

Fig. 7. Dependence of OSL signal on the readout temperature

The following test sequences were used:

1. Irradiation of each sample with a dose of 300 mGy;
2. Preheating at 140°C (heating rate 5°C/s) for 10 s;
3. OSL stimulation at T_{Roi} °C (heating rate 5°C/s) for 40 s;
4. Repeating sequences (1) to (3) from TRo1=100 °C with increasing readout temperature T_{Roi} by 25°C.

From OSL signals obtained, the readout temperature (T_{Ro}) is selected for which the signal has the highest intensity and

the lowest decay rate. In this case, it is the temperature of 100°C.

The dose response determined using a single-aliquot regenerative dose methodology on five samples is shown in Figure 8, with the maximum deviation from the set dose (1 Gy) at less than 10%.

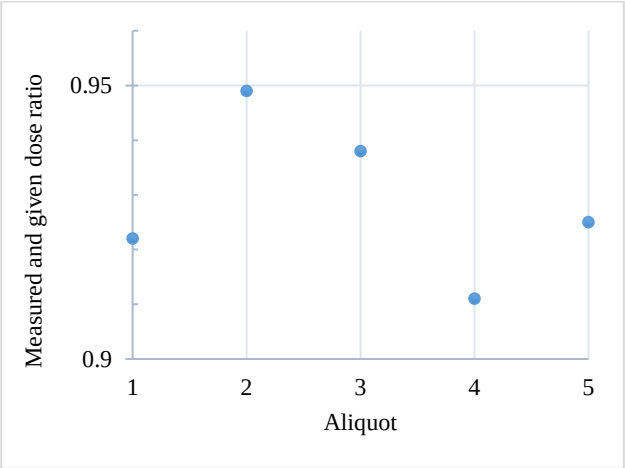

Fig. 8. SAR measurement of for dose recovery test for a laboratory given accident dose of 1 Gy.

An example of deconvolution results is shown in Figure 9. The thick solid line shows the best fit curve of experimental results (crosses), and the thin solid lines represent peaks used for deconvolution.

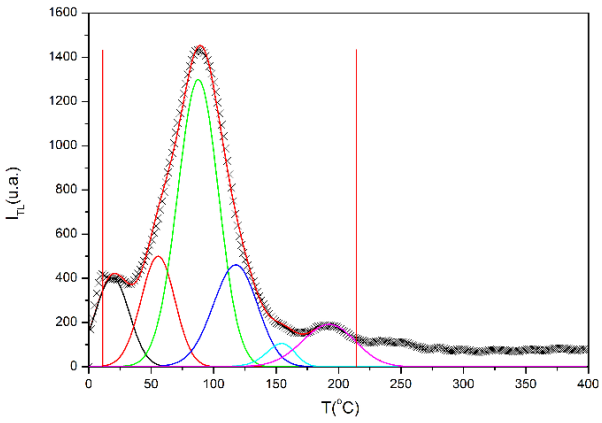

Fig. 9. Fitted glow curve by deconvolution with the TL/OSL glow curve analyzer

This study was developed using six peaks, taking into account the First Order Kinetic (FOK) approach and the continuous trap distribution (using the Gaussian expression).

Deconvolution results are summarized in Table 1. These results include activation energy E, intensity of the maximum I_{max}, temperature of the maximum T_{max}, and frequency factor σ.

TABLE I
KINETIC PARAMETERS OBTAINED BY DECONVOLUTION

	E (eV)	I_{max} (a.u.)	T_{max} (°C)	σ
Peak I	1.36	393.03	21.65	0.058
Peak II	1.61	488.08	58.29	0.059
Peak III	1.64	1265.76	91.01	0.067
Peak IV	1.48	447.98	121.41	0.057
Peak V	1.93	103.65	156.32	0.034
Peak VI	1.83	186.11	196.91	0.072

IV. CONCLUSION

Luminescence properties of common salt (NaCl) widely used on the open Macedonian market were investigated. A protocol with measurement procedures that can be used to determine luminescent properties of materials for application in retrospective dosimetry was applied. First, TL/OSL response of an irradiated and non-irradiated sample was investigated, with satisfactory results obtained. From examination of the dose response, linear response was obtained for the entire examined area. This material was identified as having potential for use in retrospective dosimetry. Preheating and reading temperatures were determined, to which SAR method for dose determination was applied, yielding high accuracy results.

ACKNOWLEDGEMENT

Authors would like to thank Faculty of Electrical Engineering and Information Technologies for funding the project Retrospective dosimetry in incidents – RETRODOSE, from which this research has resulted.

REFERENCES

[1] Bailey, R. M.; Adamiec, G.; Rhodes, E. J. OSL. "Properties of NaCl Relative to Dating and Dosimetry". Radiat. Meas. 2000, 32 (5), 717–723. https://doi.org/https://doi.org/10.1016/S1350-4487(00)00087-1.

[2] Okada, G.; Motoki, S.; Sakamoto, M.; Kusano, E.; Yada, R.; Fujimoto, Y.; Yanagida, T.; Nanto, H. "Characterization of Optically-Stimulated Luminescence Properties by NaCl:Eu2+ Crystal and the Thermal Response". J. Alloys Compd. 2021, 863, 158561. https://doi.org/https://doi.org/10.1016/j.jallcom.2020.158561.

[3] Datz, H.; Druzhyna, S.; Oster, L.; Orion, I.; Horowitz, Y. "Study of the Suitability of Israeli Household Salt for Retrospective Dosimetry". Radiat. Prot. Dosimetry 2016, 170 (1–4), 407–411. https://doi.org/10.1093/rpd/ncv517.

[4] Alghamdi, H.; Sanderson, D.; Carmichael, L.; Cresswell, A.; Martin, L. "The Use of Portable OSL and IRSL Measurements of NaCl in Low Dose Assessments Following a Radiological or Nuclear Emergency". Frontiers in Public Health, 2022.

[5] Majgier, R.; Rääf, C. L.; Mandowski, A.; Bernhardsson, C. "OSL Properties in Various Forms of KCl and NaCl Samples after Exposure to Ionizing Radiation". Radiat. Prot. Dosimetry 2019, 184 (1), 90–97. https://doi.org/10.1093/rpd/ncy189.

[6] Ademola, J. A. "Luminescence Properties of Common Salt (NaCl) Available in Nigeria for Use as Accident Dosimeter in Radiological Emergency Situation". J. Radiat. Res. Appl. Sci. 2017, 10 (2), 117–121. https://doi.org/https://doi.org/10.1016/j.jrras.2017.01.003.

[7] Szufa, K. M.; Majgier, R. "Optically Stimulated Luminescence Properties of Commercially Available KCL Dietary Supplements as

Retrospective Dosimeters". Luminescence 2022, n/a. https://doi.org/https://doi.org/10.1002/bio.4355.

[8] Bernhardsson, C.; Christiansson, M.; Mattsson, S.; Rääf, C. L. "Household Salt as a Retrospective Dosemeter Using Optically Stimulated Luminescence". Radiat. Environ. Biophys. 2009, 48 (1), 21–28. https://doi.org/10.1007/s00411-008-0191-y.

[9] Fujita, H.; Jain, M.; Murray, A. S. "Utilization of OSL from Table Salt in Retrospective Dosimetry". Japanese J. Heal. Phys. 2011, 46, 60–65.

[10] Fuochi, P.; Alberti, A.; Bortolin, E.; Corda, U.; Civita, S. La; Onori, S. "PSL Study of Irradiated Food: NaCl as Possible Reference Material". Radiat. Meas. 2008, 43, 483–486.

[11] Roman-Lopez, J.; Piña López, Y. I.; Cruz-Zaragoza, E.; Marcazzó, J. "Optically Stimulated Luminescence of Natural NaCl Mineral from Dead Sea Exposed to Gamma Radiation". Appl. Radiat. Isot. 2018, 138, 60–64. https://doi.org/https://doi.org/10.1016/j.apradiso.2017.05.001.

[12] Spooner, N. A.; Smith, B. W.; Creighton, D. F.; Questiaux, D.; Hunter, P. G. "Luminescence from NaCl for Application to Retrospective Dosimetry". Radiat. Meas. 2012, 47 (9), 883–889. https://doi.org/10.1016/j.radmeas.2012.05.005.

[13] Spooner, N. A.; Smith, B. W.; Williams, O. M.; Creighton, D. F.; McCulloch, I.; Hunter, P. G.; Questiaux, D. G.; Prescott, J. R. "Analysis of Luminescence from Common Salt (NaCl) for Application to Retrospective Dosimetry". Radiat. Meas. 2011, 46 (12), 1856–1861. https://doi.org/10.1016/j.radmeas.2011.06.069.

[14] Tanir, G.; Bolukdemir, M. H. "Infrared Stimulated Luminescence-Decay Shape from NaCl as a Function of Radiation Doses". Radiat. Meas. 2007, 42 (10), 1723–1726. https://doi.org/10.1016/j.radmeas.2007.07.003.

[15] Benavente, J.F.; Gómez-Ros, J.M; Romero, A.M. "Thermoluminescence Glow Curve Deconvolution for Discrete and Continuous Trap Distributions". Applied Radiation and Isotopes. 2019, 153. https://doi.org/10.1016/j.apradiso.2019.108843.

Journal of Electrical Engineering and Information Technologies, Vol. **9**, No. 2 pp. 87-92 (2024)
Article 222
Received: May 20, 2024
Accepted: November 10, 2024
In print: ISSN 2545–4250
Online: ISSN 2545–4269
UDC: 621.313.333.013.6
doi.org/10.51466/JEEIT2492222087t

Original Scientific Paper

THE IMPACT OF HIGH ORDER HARMONICS OF SUPPLY VOLTAGE ON OPERATING CHARACTERISTICS OF INDUCTION MOTORS

Ivan Temelkovski[1)] Goran Rafajlovski Mihail Digalovski Krste Najdenkoski

Ss. Cyril and Methodius University in Skopje, Faculty of Electrical Engineering and Information Technologies
1000 Skopje, Macedonia

[1)] ivant@feit.ukim.edu.mk

Abstract: This paper considers the impact of high order harmonics on efficiency, power factor (PF), stator current, and electromagnetic torque developed by a three-phase induction cage motor. In that regard, three cases are examined in detail: the first - when the induction motor is connected to sinusoidal voltage, the second - when the induction motor is connected to voltage that contains high order harmonics (second and third order) despite the fundamental harmonic, and the third - when the induction motor is connected to voltage that contains both, i.e. fundamental and third order harmonic. Based on the simulation created in the Matlab SIMULINK programming and numeric platform, an analysis was made of each of the three cases, clearly highlighting the differences observed. The main aim of this paper is to make a comparison and estimate the error that could be made by neglecting the presence of one of the supply voltage high order harmonics for the induction motor, as well as to highlight the importance of taking these harmonics into account in calculations for operating characteristics of induction machines.

Keywords: high order harmonics, efficiency, induction motor

ВЛИЈАНИЕТО НА ВИШИТЕ ХАРМОНИЦИ НА ПРИКЛУЧНИОТ НАПОН ВРЗ РАБОТНИТЕ КАРАКТЕРИСТИКИ НА АСИНХРОНИТЕ МОТОРИ

Апстракт: Овој труд го разгледува влијанието на вишите хармоници врз коефициентот на полезно дејство, факторот на моќност, статорската струја и врз електромагнетниот момент што го развива трифазен асинхрон мотор со кафезен ротор. Притоа, детално се разгледани три случаи: еднаш - кога асинхрониот мотор е приклучен на чист синусен напон, вторпат - кога асинхрониот мотор е приклучен на напон кој содржи виши хармонци од втор и од трет ред и третпат - кога асинхрониот мотор е приклучен на напон кој го содржи основниот и третиот хармоник. Врз основа на симулацијата што е изработена во програмата Матлаб СИМУЛИНК, направена е анализа на секој од случаите, при што јасно се истакнати разликите што се забележуваат. Главната цел на овој труд е да се направи споредба и да се процени грешката што би се направила доколку во одредени случаи се занемари присуството на некој од вишите хармоници на приклучниот напон на асинхрониот мотор, како и да се истакне важноста од земањето предвид на овие хармоници во пресметките на работните карактеристики на моторите.

Клучни зборови: виши хармоници, ефикасност, асинхрон мотор.

I. INTRODUCTION

Induction motors are rotating electrical machines that should be used at rated frequency and sinusoidal form of voltage and load current. However, due to the increasing number of inverter-fed induction motors and feedback effects of the grid, there is no doubt that the analysis of the impact of high voltage and current harmonics on efficiency, power factor, and power losses of induction motors holds great importance. That is one of the main reasons why it is of crucial importance for significant harmonics to be taken into account when determining operating characteristics of induction motors [7].

In general, based on the direction of the magnetic fields produced by the harmonics, all harmonics occurring in the supply voltage can be divided into three groups [6]:

- positive;
- negative;
- zero sequence harmonics.

It should be noted that positive sequence harmonics (1,4,7, etc.) produce magnetic fields and currents rotating in the same direction as the fundamental frequency harmonic. On the other side, negative sequence harmonics (2,5,8, etc.) produce magnetic fields and currents that rotate in direction opposite to the fundamental frequency harmonic. Finally, zero sequence harmonics (3,9,15, etc.)

do not produce usable torque, but additional losses in the machine [12].

As a result of interaction between positive and negative sequence magnetic fields and currents, torsional oscillations of the motor shaft can be generated, leading to shaft vibrations that result in huge damage to the motor.

II. Mathematical Model Of Induction Motor

According to Fourier analysis, it is well-known that any non-sinusoidal waveform can be given as a sum of multiple sine waveforms with different frequency. In that respect, non-sinusoidal voltages and currents can be expressed as [10]:

$$v(t) = \sqrt{2}[V_1 \sin \omega_0 t + \sum_{k=2}^{\infty} V_k \sin(k\omega_0 t + \varphi_k)] \quad (1)$$

$$i(t) = \sqrt{2}[I_1 \sin \omega_0 t + \sum_{k=2}^{\infty} I_k \sin(k\omega_0 t + \theta_k)] \quad (2)$$

where:
V_1, I_1 are fundamental voltage and current;
V_k, I_k are k^{th} order harmonic voltage and current;
φ_k, θ_k are phase angles of k^{th} order harmonic voltage and current; and
ω_0, is radian frequency of the fundamental wave.

According to relevant IEEE standards, the total voltage harmonics distortion factor (THD-*U*) is defined as:

$$THD_U(\%) = \sqrt{\frac{\sum_{k=2}^{\infty} V_k^2}{V_1^2}} \times 100\% \quad (3)$$

and the amount of voltage distortion due to k^{th} order harmonic is measured by the voltage distortion factor (*VDF*) as [10]:

$$VDF(\%) = \frac{V_k}{V_1} \times 100\% \quad (4)$$

On the other side, the total current harmonics distortion factor (THD-*I*) is defined as:

$$THD_I(\%) = \sqrt{\frac{\sum_{k=2}^{\infty} I_k^2}{I_1^2}} \times 100\% \quad (5)$$

III. Simulink Model Of Induction Motor

In order to make qualitative and quantitative analysis of the impact of high order harmonics on operating characteristics of induction motors, a Simulink model was created, as shown in Figure 1.

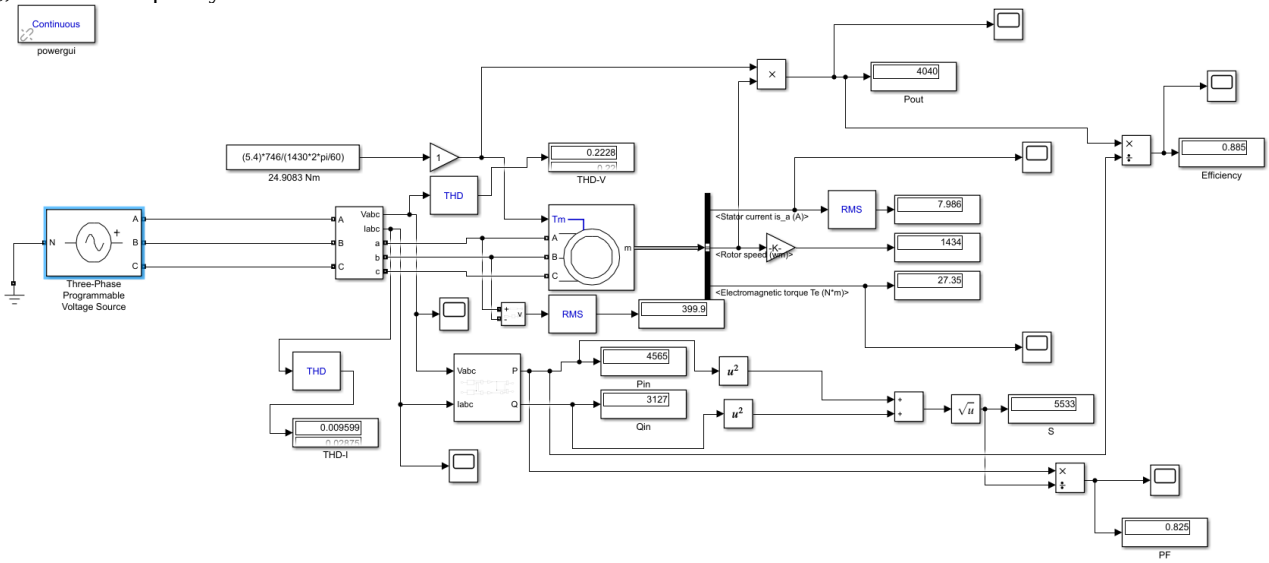

Fig. 1. Simulink model of induction motor

The analysis considered a three-phase induction squirrel-cage induction motor: P_n=4 kW, U_n=400 V, n_n=1430 rpm, f_n=50 Hz.

The block from Simscape library named "Three Phase Programmable Voltage Source" was used as a three-phase voltage source. This block implements a three-phase zero-impedance voltage source. Time variation for amplitude, phase, and frequency of the fundamental can be preprogrammed. In addition, two harmonics can be superimposed on the fundamental.

In order to measure the active and reactive power that the motor takes from the grid, a power block is also used, ensuring measurement of instantaneous active and reactive power.

It should be noted that each of the blocks is adapted to nominal parameters of the induction motor considered.

Table I provides an overview of general data for each of the harmonics taken into account during the analysis, such as amplitude of the harmonic in terms of the fundamental harmonic, its order, and sequence of the harmonics.

TABLE I
General Data Of Harmonics

Order of harmonics (h)	Amplitude (pu)	Phase (degrees)	Sequence
1	1	0	Positive
2	0.15	35	Negative
3	0.22	-25	Zero

IV. Results And Discussion

A. Total Harmonic Distortion

Based on the Matlab simulation of an induction motor, results were obtained for the total harmonic voltage and current distortion. Data presented in Table II show the values of the total harmonic voltage (THD-U) and current (THD-I) distortion, respectively.

TABLE II
TOTAL HARMONIC VOLTAGE AND CURRENT DISTORTION

Order of harmonics (h)	**1**	**1 and 3**	**1,2 and 3**
THD-U	0.0062	0.2228	0.2678
THD-I	$1.49 \cdot 10^{-8}$	0.009599	0.5724

It can be noted that the presence of harmonics significantly affects the total harmonic distortion, making it clear that they should not be neglected in calculations. The presence of both harmonics (2nd and 3th) greatly worsens the total harmonic distortion, which can be one of the main reasons for additional power losses that occur in induction machines. The value of the total voltage harmonic distortion when all harmonics are taken into account is 43.19 times higher than its value when they are neglected.

If the impact of the second harmonic is neglected, the total harmonic voltage distortion will be reduced by only 1.17 times, signifying that no significant error occurs.

B. Efficiency and Power Factor

TABLE III
EFFICIENCY AND POWER FACTOR (PF)

Order of harmonics (h)	**1**	**1 and 3**	**1,2 and 3**
Efficiency (%)	88.5	88.5	88.32
Power Factor (PF)	0.825	0.825	0.8264

It should be noted that this paper puts the emphasis on the impact of the second and third harmonics, and since harmonics of this order usually have a larger amplitude compared to harmonics of higher orders, it is clear that their influence cannot be neglected.

Values for the induction motor's efficiency and power factor for each of the cases considered are given in Table III. It can be seen that these values do not differ greatly for each of the cases considered, making it clear that they can be neglected in some cases.

C. Stator Current of Induction Motor

It is known that the fundamental component of the stator current is determined by the motor load and therefore it is clear that the relative harmonic content of the motor current is significantly higher at lower than at higher loads. This high harmonic content can cause a significant increase in power losses in unloaded machine, compared to its values when the machine is connected to sinusoidal voltage [12].

If V_k denotes the k^{th} harmonic component of the supply voltage, the corresponding stator current harmonic is $I_k=V_k/Z_k$, where Z_k is the k^{th} harmonic input impedance. For positive- and negative-sequence harmonics, $Z_k=k(X_1+X_2)$. Thus:

$$I_k = \frac{V_k}{k(X_1 + X_2)} \tag{6}$$

for zero-sequence harmonics, $Z_k=kX_0$; and

$$I_k = \frac{V_k}{kZ_0} \tag{7}$$

These formulas allow rapid evaluation of harmonic currents due to non-sinusoidal voltage waveform with known harmonic content. Usually, there are no zero-sequence harmonics and no even-numbered harmonics, thus the total rms harmonic current is given by [10]:

$$I_h = \sqrt{I_5^2 + I_7^2 + I_{11}^2 + I_{13}^2 + ... + I_k^2 + ...} \tag{8}$$

$$I_h = \sqrt{\sum_{k \neq 1} I_k^2} \tag{9}$$

If I_{rms} denotes the motor's fundamental root mean square (rms) current, it is clear that the total rms stator current, including the fundamental, can be calculated as [10]:

$$I_{rms} = \sqrt{I_1^2 + I_5^2 + I_7^2 + I_{11}^2 + I_{13}^2 + ... + I_k^2 + ...} \tag{10}$$

$$I_{rms} = \sqrt{I_1^2 + I_{har}^2} \tag{11}$$

It can be noted that, for a given voltage waveform, the relative harmonic content of the stator current is closely related to the motor's leakage reactance. In calculations and analyses, it is very practical to express the motor current, as well as the leakage reactance, in normalized or per-unit form (pu). They actually represent a ratio between the actual value of current or reactance and their base values.

The k^{th} harmonic current can be expressed in per-unit form as fraction of the rated full-load current. Thus:

$$I_k = \frac{V_k}{kX_{pu}} \tag{12}$$

where V_k is now the per-unit k^{th} harmonic voltage based on the rated sine wave voltage of the motor.

For operation at rated frequency, X_{pu} is the normal per-unit leakage reactance parameter of the motor, but obiously this reactance varies linearly with frequency. It is convenient to retain X_{pu} as the per-unit reactance at rated or base frequency and to take into account the frequency dependence of leakage reactance by means of a multiplying factor f_1, which is the per-unit fundamental frequency, and has value 1 at rated motor frequency. The k^{th} harmonic per-unit current at a per-unit fundamental frequency, f_1, is then given by:

$$I_k = \frac{V_k}{kf_1X_{pu}} \tag{13}$$

For the six-step voltage waveform, the magnitude of each harmonic voltage is inversely proportional to the order of the harmonic. Thus:

$$V_k = \frac{V_1}{k} \tag{14}$$

and if this expression is substituted in equation (13), the following expression can be obtained:

$$I_k = \frac{V_1}{k^2 f_1 X_{pu}} \tag{15}$$

Fundamental airgap flux is directly proportional to stator induced electromotive force (emf), E_1, and inversely proportional to frequency. In order to obtain a good approximation, except at low frequency, airgap flux is therefore proportional to V/f. If the base value of airgap flux is that corresponding to the rated terminal voltage, V_R, at rated frequency, f_R, then the per-unit fundamental airgap flux can be expressed as:

$$\Phi_1 = \frac{V_1}{f_1} \tag{16}$$

where V_1 and f_1 are also expressed in per-unit form.

If the voltage V_1 is expressed from equation (16) and if this value is substituted in equation (15), the k[th] harmonic of the current can be obtained:

$$I_k = \frac{\Phi_1}{k^2 X_{pu}} \tag{17}$$

At normal conditions, i.e. with constant volt-hertz regulation, the base frequency Φ_1 is unity, so now the equation can be written as:

$$I_k = \frac{1}{k^2 X_{pu}} \tag{18}$$

Since X_{pu} is the per-unit reactance at base frequency, it is evident that harmonic current amplitudes are independent of supply frequency and motor load if the volts/hertz ratio is constant.

Figure 2 shows the stator current flowing through one of the phase windings. Figure 2a shows the waveform of the stator current when high order harmonics are neglected. On the other side, Figure 2b shows the stator current waveform when high order harmonics are taken into account. At the same time, it should be noted that the current largely deviates from its sinusoidal shape in the cases when the harmonics of the supply voltage are not neglected, which leads to increased power losses in the induction motor's windings. Based on the graphic, it can also be observed that the initial value of the motor inrush current is almost no different for each of the cases considered.

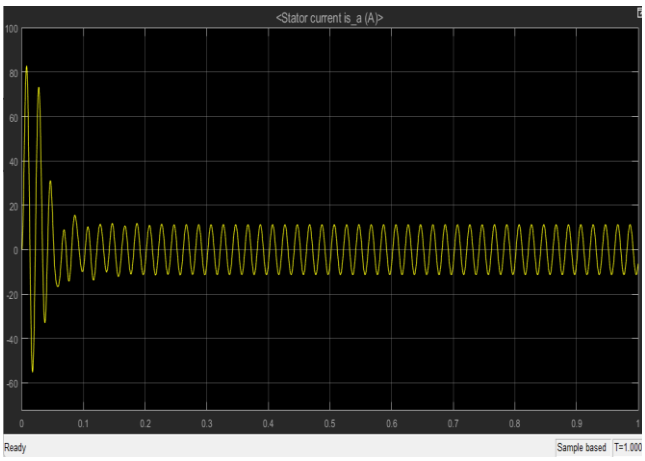

(a)

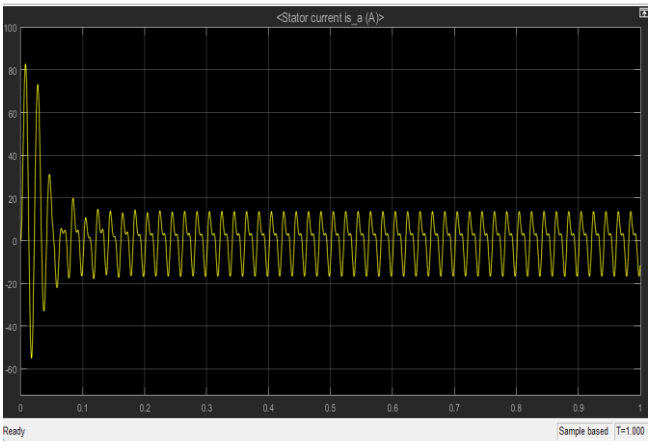

(b)

Fig. 2. Stator current of induction motor: a) when high order harmonics are neglected, b) when high order harmonics are not neglected

D. Electromagnetic Torque

On the other hand, Figure 3 shows the electromagnetic torque developed by the induction motor. Figure 3a shows the electromagnetic torque assuming higher harmonics are neglected, while Figure 3b shows the electromagnetic torque of the induction motor taking into account higher harmonics.

It can be seen that in the cases when the higher harmonics are not neglected, the torque gets a constant value, but this is not the case when the high order harmonics are present [12].

The presence of time harmonic magnetomotive force (mmf) waves in the airgap results in additional harmonic torques on the rotor. These torques can be divided into two groups: steady harmonic torques and pulsating harmonic torques.

Constant or steady torques are developed by the reaction of harmonic airgap fluxes with harmonic rotor mmfs, or currents, of the same order. However, these steady harmonic torques, which are a very small fraction of rated torque, have negligible effect on motor operation. This may be verified by calculating the torque contribution from the harmonic equivalent circuit, just as fundamental torque is derived from the fundamental equivalent circuit. Thus, the fundamental torque is given as:

$$T_1 = \frac{pm_1}{2\pi f_1} I_2^2 \frac{R_2}{s_1} \tag{19}$$

Similarly, based on the corresponding electrical equivalent circuits for each of the harmonics, the following expression can be rewritten for the k[th] harmonic of the moment:

$$T_k = \pm \frac{pm_1}{2\pi k f_1} I_{2k}^2 \frac{R_{2k}}{s_k} \tag{20}$$

where forward torque due to a positive-sequence harmonic is positive and backward torque due to a negative-sequence harmonic is negative.

The fundamental slip, s_1, is small for normal full-load operation of the induction motor, and consequently the following expression can be written for the harmonic slip [12]:

$$s_k = \frac{k \mp 1}{k} \tag{21}$$

Substitution in equation (20) gives the following:

$$T_k = \pm \frac{pm_1}{2\pi f_1} I_{2k}^2 \frac{R_{2k}}{k \mp 1} \tag{22}$$

Thus, the k[th] harmonic torque, expressed as a fraction of the fundamental torque, is:

$$\frac{T_k}{T_1} = \pm \left(\frac{I_{2k}}{I_2} \right)^2 \left(\frac{R_{2k}}{R_2} \right) \left(\frac{s_1}{k \mp 1} \right) \tag{23}$$

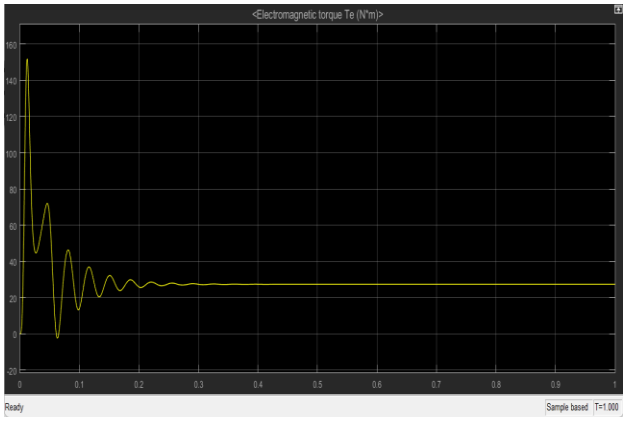

(a)

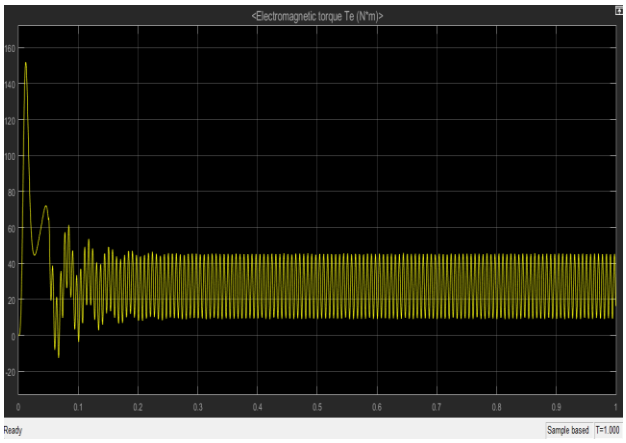

(b)

Fig. 3. Electromagnetic torque: a) when high order harmonics are neglected, b) when high order harmonics are not neglected

If the motor operates at rated load, then I_2 is near rated current and (I_{2k}/ I_2) is approximately equal to the per-unit k[th] harmonic of the current, as given in equation (13). Substituting this expression in equation (23) gives the general equation:

$$\frac{T_k}{T_1} = \pm \left(\frac{V_k}{k f_1 X_{pu}} \right)^2 \left(\frac{R_{2k}}{R_2} \right) \left(\frac{s_1}{k \mp 1} \right) \tag{24}$$

In the case of a six-step voltage waveform, the per-unit value of I_k, is given by equation (17), and substituting I_{2k}/I_2, in equation (23) gives the corresponding harmonic torque equation as:

$$\frac{T_k}{T_1} = \pm \left(\frac{\Phi_1}{k^2 X_{pu}} \right)^2 \left(\frac{R_{2k}}{R_2} \right) \left(\frac{s_1}{k \mp 1} \right) \tag{25}$$

where Φ_1 is the per-unit airgap flux, as defined in equation (16).

Now consider the fifth harmonic torque in the case of an induction motor operating on a six-step voltage supply. Rated fundamental voltage and frequency are applied so that Φ_1 is unity.

Let it be assumed that the resistance of the rotor winding is three times greater as a result of the skin effect, while the slip value of the fundamental harmonic is 0.03. The relation between the moment for the fifth and the fundamental harmonic can be written as:

$$\frac{T_5}{T_1} = \frac{-0{,}24 \cdot 10^{-6}}{X_{pu}^2} \tag{26}$$

Thus, for a leakage reactance of 0.1 pu, it can be shown that T_5 is 0.24 percent of the fundamental torque. For a leakage reactance of 0.2 pu, T_5 is only 0.06 percent of T_1. This small counter-torque due to the negative-sequence fifth harmonic is opposed by a somewhat smaller forward torque due to the positive-sequence seventh harmonic. The combined effect of the fifth and seventh harmonics is, therefore, to produce a very small negative torque opposing the fundamental motor torque.

On the other side, the pulsating torques are produced as result of interaction between mmfs for each of the harmonics of the rotor and rotating magnetic fluxes for the harmonics of different order. Since the magnetic fluxes in the air gap for each of the harmonics have small values, it is clear that the dominant pulsating moments are actually the result of interaction between the rotor currents (or magnetomotive forces) and the fundamental rotating magnetic flux. For example, the fifth harmonic of the stator currents forms a system of inverse order and, at the same time, for the fundamental harmonic, creates a space wave of the magnetic voltage that rotates at a speed five times greater than the fundamental synchronous speed, but in the direction opposite to that of the fundamental magnetic field.

The rotor currents produced by this time harmonic of the magnetic field interact with the fundamental rotating magnetic field, creating a pulsating torque whose frequency is six times greater than the fundamental, as a result of the fact that the speed of the rotor mmf waveform for the corresponding harmonic in the air gap compared to the fundamental magnetic field in the airgap is actually six times greater than the synchronous speed of the fundamental field. The seventh harmonic of the stator current also creates a pulsating torque whose frequency is six times greater than the fundamental. The order of the seventh harmonic is direct (positive) and therefore this harmonic creates a time harmonic of the rotating magnetic field with a seven times greater speed than the synchronous, in the same direction as that of the fundamental magnetic field.

Again, it can be noted that the relative velocity of the mmf waveform for the corresponding harmonic compared to the fundamental magnetic field in the air gap is six times greater than the synchronous velocity, but this time in the opposite direction. It can be concluded that the mean value of the pulsating torques is 0, but their presence creates an angular velocity of the rotor that changes during rotation. At very low speeds, motor rotation occurs in interrupted or stepped motions, and this cannot be tolerated in some applications.

When some high order voltage harmonics are applied to an induction motor, it can result in production of pulsating torque as a result of interaction between the harmonics and

the motor's rotor slots. There is no doubt that the presence of non-sinusoidal voltage component can impact smooth rotation of the induction motor and this should not be neglected during construction of induction motors.

V. Conclusion And Future Work

Based on results and facts presented, it is not difficult to conclude that high order harmonics have a huge impact on several parameters of induction motors. That is one of the main reasons that sometimes lead to a number of possible side effects, such as mechanical damage or aging of induction motors. The extent to which these damages occur can be subject of further analysis and design of a solution to address these problems. In the end, it should be highlighted that, in all cases when the results obtained from this paper will be taken into account, industrial companies would clearly pay attention to the process of selecting the right electrical motor for their applications, thus increasing both economy and positive effect on the environment.

References

[1] Ashish Kamal, V. K. Giri. "Mathematical Modelling of Dynamic Induction Motor and Performance Analysis with Bearing Fault". IJITR, Volume 01, Issue – 04. June/July 2013.

[2] Sifat Shah, A. Rashid, MKL Bhatti. "Direct Quadrate (DQ) Modelling Of 3-Phase Induction Motor Using Matlab/Simulink". Canadian Journal of Electrical and Computer Engineering, Vol.3, No.5. May 2012.

[3] B. Ozpineci, L. M. Tolbert. "Sim Machine Model –A Modular Approach". IEEE, 2, pp.728-734.

[4] Er. Yogesh, G. Tayade, B.S. Dani, K. B. Porate. "Mathematical Modeling 15kW Standard Induction Motor Using MATLAB/SIMULINK". IJSRD - International Journal for Scientific Research & Development, Vol.1, Issue 9, 2013 ISSN (online): 2321-0613.

[5] Adrián Bolaño Martínez, Isaac Jiménez Navarro, Vladimir Sousa, Enrique Ciro Quispe, Pablo Donolo. "MATLAB/Simulink Modeling of Electric Motors Operating with Harmonics and Unbalance". International Journal of Electrical and Computer Engineering (IJECE) Vol.12, No.5, October 2022, pp. 4640~4648, ISSN: 2088-8708, DOI: 10.11591/ijece.v12i5.pp 4640-4648.

[6] Horia Gheorghe Beleiu, Virgil Maier,Sorin Gheorghe Pavel, Iulian Birou, Constantin Sorin Pică and Pompei Cosmin Dărab. "Harmonics Consequences on Drive Systems with Induction Motor". Applied Science, February 24, 2020.

[7] Mirzapour, O., Karimi-Arpanahi, S., Oraee, H. "Evaluating Grid Harmonics Effect on Induction Motor Using Reduced Thermal Model" in proceedings of the 2018 Smart Grid Conference (SGC), Sanandaj, Iran, November 18-29, 2018; pp. 1–5.

[8] Agamloh, E., Peele, S., Grappe, J. "An Experimental Evaluation of the Effect of Voltage Distortion on the Performance of Induction Motors", in proceedings of the Conference Record of 2012 Annual IEEE Pulp and Paper Industry Technical Conference (PPIC), Portland, OR, USA, June 17-21, 2012; pp. 1–7.

[9] M. Jiang, J. Tian, H. Hwang Goh, J. Yi, S. Li, D. Zhang, T. Wu. "Experimental Study on the Influence of High Frequency PWM Harmonics on the Losses of Induction Motor", 2022 International Conference on Energy Storage Technology and Power Systems (ESPS 2022), February 25–27, 2022, Guilin, China.

[10] Otýpka J., Pečínka P., Orság P., Stýskala V. "The Influence of Nonharmonic Voltage Source on Losses in Induction Motor", Conference Paper 2017, DOI: 10.1109/EPE.2017.7967246.

[11] L. Tomasz and R. Michal. "Influence of Higher Harmonics on Losses in Induction Machines", Technical Transactions: Electrical Engineering, DOI: 10.4467/2353737XCT.16.262.6061.

[12] J. M. D.Murphy, F. G. Turnbull. "Power Electronic Control of AC Motors", Pergamon Press, 1989.

Journal of Electrical Engineering and Information Technologies, Vol. **9**, No. 2 pp. 93-99 (2024)
Article 223
In print: ISSN 2545–4250
Received: June 20, 2024
Online: ISSN 2545–4269
Accepted: November 15, 2024
UDC: 502.3:504.5]:621.313.076.7(497.7)
doi.org/10.51466/JEEIT2492223092m

Original Scientific Paper

MITIGATING AIR POLLUTION IN NORTH MACEDONIA: THE ROLE OF POWER ELECTRONICS IN ENERGY GENERATION AND CONSUMPTION

Slobodan Mirčevski[1)] Goran Rafajlovski[2)] Mikołaj Bartłomiejczyk [3)] Ivan Temelkovski[4)]

[1,2,4] Ss. Cyril and Methodius University in Skopje, Faculty of Electrical Engineering and Information Technologies 1000 Skopje, Macedonia, [3]South Western University, [3] Faculty of Electrical and Control Engineering, Gdansk University of Technology, Gdansk, Poland

[1)] mirceslo@feit.ukim.edu.mk

Abstract: Environmental pollution and global warming are the greatest world problems today. Climate change and global warming (1.4 ˚C in 2023) as an issue of human survival on the planet Earth are a direct consequence of pollution. Environmental pollution should be divided into air pollution, water pollution, and soil contamination. This paper considers only air pollution in the Republic of North Macedonia and possible solutions thereto. All pollution types are a result of human habits, industrialization and the need for energy sources. Although the greatest environmental pollution comes from developed countries, the most polluted towns are easily found in underdeveloped countries, mainly as a result of poor standards, inadequate heating, and traffic using old buses, cars, etc. The impact of power electronics in industrialization and energy generation is very significant, and therefore it could be equally important for finding a solution to the problem. Power electronics are necessary not only for classical types of power plants (coal, hydro, oil, gas, and nuclear), but even more for renewable power sources such as wind farms, small hydropower plants, and solar plants. The industry is the greatest consumer of electricity, with electric drives accounting for two thirds of that consumption. Households are the second biggest consumer of electricity, with electric drives such as air conditioners and other HVAC (Heating, Ventilation, Air Conditioning) systems, washing machines, refrigerators, dust cleaners, and auxiliary domestic tools having a dominant share. Power electronics is a structure block of any contemporary electric drive and the best way to improve energy efficiency and reduce electricity consumption. On the other hand, they imply less need for electricity. Electric transport is a powerful way to reduce CO_2 emissions. High power fans with filters are necessary for air cleaning at power plants and industrial facilities. Water cleaning is done with the help of purification stations with pumps. In all these cases, power electronics for variable speed drives are used. High-efficiency motors (HEM) are already in use and contribute to lower electricity consumption.

Keywords: air pollution, power electronics, electricity, generation, consumption

ПОДОБРУВАЊЕ НА СОСТОЈБАТА СО ЗАГАДУВАЊЕТО НА ВОЗДУХОТ ВО МАКЕДОНИЈА: УЛОГАТА НА ЕНЕРГЕТСКАТА ЕЛЕКТРОНИКА ВО ПРОИЗВОДСТВОТО И ПОТРОШУВАЧКАТА НА ЕЛЕКТРИЧНА ЕНЕРГИЈА

Апстракт: Загадувањето на животната средина и глобалното затоплување се најголемите проблеми со кои светот се соочува денес. Климатските промени и глобалното затоплување (1,4 ˚C во 2023 година) како прашање за опстанокот на човекот на планетата Земја се последица токму на загадувањето. Загадувањето на животната средина може да се подели на загадување на воздухот, загадување на водата и контаминација на почвата. Во овој труд се разгледува само загадувањето на воздухот во Република С. Македонија и можните решенија. Сите типови загадувања се резултат на човечките навики, индустријализацијата и на потребата од извори на енергија. Иако најголемото загадување на животната средина потекнува од најразвиените земји, најзагадените градови се лоцирани во нискоразвиените земји, како резултат на лош стандард, несоодветно греење и сообраќај со стари автобуси, автомобили, итн. Влијанието на енергетската електроника во индустријализацијата и производството на енергија е многу значајно, па оттука може да биде многу важно за решавање на проблемот. Енергетската електроника е неопходна не само за класичните типови електрични централи (термо, хидро, гасни и нуклеарни), туку уште повеќе за обновливите извори на електрична енергија како што се ветерниците, малите хидроцентрали и соларните централи. Индустријата е најголемиот потрошувач на електрична енергија и во неа учествуваат електромоторните погони со 2/3. Домаќинствата се вториот голем потрошувач на електрична енергија бидејќи во него доминантно влијание имаат електромоторните погони како што се клима уредите и другите слични уреди (за греење, за вентилација, за климатизација), машините за перење, фрижидерите, електричните уреди за чистење прашина и помошни домашни уреди. Енергетската електроника влегува во склоп на секој современ електроморотен погон и е најдобриот начин за подобрување на енергетската ефикасност и намалување на потрошувачката на електрична енергија. Од друга страна, тоа значи помала потреба од електрична енергија. Електричниот транспорт е моќен начин за намалување на емисиите на CO_2. Вентилаторите со голема моќност со филтри се неопходни за чистење на воздухот во електраните и во индустриите. Чистењето на водата се врши со

помош на пречистителни станици со пумпи. Во сите овие случаи се користи енергетска електроника за погони со променлива брзина. Моторите со висока ефикасност се веќе во употреба и придонесуваат за намалена потрошувачка на електрична енергија.

Клучни зборови: загадување на воздухот, енергетска електроника, електрична енергија, производство, потрошувачка.

I. INTRODUCTION

CIVILIZATION development is tightly connected with technological progress and improvement. In that process, people often forget about consequences on the nature's behavior and that they must live in harmony with the nature. Use of nature wealth (water, earth for food-producing, wood, minerals, etc.) should be very carefully and strongly planned. Man is always in battle with the nature's temper, expressed in the form of floods, droughts, forest fires, volcano activities, earthquakes, tsunamis, etc. The nature's behavior is in connection with human activities in the field of environmental pollution as unavoidable consequence of the industrialization process. Pollution of air, water, and soil contamination are all linked to energy generation and energy consumption processes. While there are many high-level global meetings and a number of international agreements in this regard, greenhouse gas emissions - GHG (expressed as CO_{2eq}) and related climate change are certainly the greatest problems of today. It is clear that the most developed industrial countries are the biggest polluters. However, the most polluted towns in the world are found in underdeveloped countries of Asia, Africa, and Europe, especially in winter, as a result of primitive heating methods, use of old buses in transport, use of old cars, low cultural, technology and industry levels. The Republic of North Macedonia is a developing country, more than 30 years of transition, with heavy environmental pollution problems and great chances to expand use of power electronics in electricity generation and consumption. This paper considers the influence of power electronics in decreasing environmental pollution. Use of power electronics in electricity generation and consumption, electric transport and electric drives is a powerful way to decrease environmental pollution [1], [2], [3], [4], [5], [7], [11], [12], [13], [14], [15], [16], [17], [18], [19], [20]. At the same time, it provides an opportunity for better, higher, and best quality goods productivity [5], [8], [9], [10], [21], [22]. Be that as it may, regular application of power electronics necessitates knowledge and advanced technology. This paper treats only air pollution, as the most dangerous pollution in North Macedonia, as well as power electronics applications in electricity generation and consumption that could greatly contribute towards a solution to the problems.

II. AIR POLLUTION IN TOWNS

Based on word statistics, towns in the Republic of North Macedonia are heavily polluted, especially in winter [6], [23], [24], [25], [26], [27], [28], [29],[30], [33]. Almost daily, the state's capital, Skopje, is featured among the top 10 most polluted towns in the world. Other towns, including Bitola, Tetovo, Strumica, Ohrid, Veles, etc., are also often featured on this list. This is due to the geographical position of towns in windless valleys, including frequent formation of fog in winter. Other reasons include low quality of living, unsuitable heating sources, use of old buses and cars, etc. It should also be noted that there are many illegal landfills with disposed waste being burned throughout the year. Waste management is still an unsolved problem, although it could serve as energy source and can be viewed as profitable business.

Air pollution is generally measured by the Air Quality Index (AQI), as shown in Table 1.

TABLE I
AIR QUALITY INDEX VALUES

Air Quality Index Levels of Health Concerns	Numerical value	Meaning
Good	0 to 50	Air quality is considered satisfactory and air pollution poses little or no risk.
Moderate	51 to 100	Air quality is acceptable, however for some pollutants there may be moderate health concerns for a very small number of people who are unusually sensitive to air pollution.
Unhealthy for sensitive groups	101 to 150	Members of sensitive groups may experience health effects. The general public is not likely to be affected.
Unhealthy	151 to 200	Everyone may begin to experience health effects. Members of sensitive groups may experience more serious health effects.
Very unhealthy	201 to 300	Health alert: everyone may experience more serious health effects.
Hazardous	301 to 500	Health warning of emergency condition. The entire population is more likely to be affected.

In addition, Table 2 provides the relation among AQI and the content of harmful materials in the air, such as particulate matters (PM10, PM2.5), 7 (seven) greenhouse gases (GHG) under the Kyoto Protocol, carbon dioxide (CO_2), methane (CH_4), nitrous oxide (N_2O), fluoride (F) gases, hydrofluorocarbons (HFCs) and perfluorocarbons (PFCs), sulfur hexafluoride (SF_6) and nitrogen three fluoride (NF_3). Sulphur dioxide (SO_2) is not GHG, but is

very dangerous when it interacts with water (rain), creating H_2SO_3. All these gases are measured per unit ($\mu g/m^3$).

For objective and practical reasons, all GHGs are presented as equivalent carbon dioxide CO_{2eq} on account of the latter's great influence, see Table 3.

TABLE II
AQI 50 IN RELATION WITH APPROPRIATE POLLUTANTS MEASURED IN RNM, [26]

AQI	PM10	PM2.5	NO_2	SO_2	CO	O_3
50	54	25	200	125	10	120

TABLE III
EQUIVALENCE AMONG GHG (SOURCE: IPCC ASSESSMENT REPORT AR4, 2007, [26])

CO_2	1
CH_4	25
N_20	298
HFC-32	675
HFC-135	3,500
HFC-134A	1,430
HFC-143A	4,470
HFC-227EA	3,220
CF_4	7,390
C_2F_6	12,200

Table 4 shows air pollution in selected towns in the Republic of North Macedonia, as measured in December 2023, with their appropriate AQI values that are close to ranges measured in the 10 most polluted towns worldwide [33].

TABLE IV
AQI IN SOME TOWNS IN RNM, DECEMBER 2023, [33]

AQI	0-50	51-100	101-150	151-200
SKOPJE	6	14	11	0
BITOLA	15	26	0	0
TETOVO	11	18	2	0
STRUMICA	6	9	14	2
OHRID	17	14	0	0
VELES	12	19	0	0

The coefficient (kg CO_{2eq}/kWh) is very useful for evaluation of air pollution in relation to the type of electricity source, whose actual value ranges from 0.3 to 2 [5]. It shows the structure of electricity sources, and in the case of fossil fuels that dominate electricity generation, its value is above 1. However, it is rarely used for measurements. Explanation of the unit 1 kg CO_2 appears necessary, as it corresponds to burning of 1kg coal or 1/2l petrol, driving a car for 3.7 km, ball with 1 m diameter full of CO_2 [23], [28].

III. THE ROLE OF POWER ELECTRONICS IN DECREASING AIR POLLUTION

A. Electricity Generation

There are no nuclear plants in the Republic of North Macedonia for power generation. Electricity generation is manly based on low quality lignite (coal), with an average calorific value of 5500 kJ/kg. Therefore, it must be enriched with oil for use in power plants. The country is fully dependent on imported oil and gas from abroad (Greece, Russia, USA, Turkey, Azerbaijan), transiting the bordering countries, i.e. Bulgaria, Greece, Albania and Serbia. Oil is necessary for road traffic, based on internal combustion engines. Use of gas is in its early stages. Most oil and gas supply is controlled by private companies. The country is developing several power and gas interconnection projects. Water sources are solid, with satisfactory quantities. Wind and photovoltaic are relatively new energy sources, with good perspectives. Many solar projects have been announced.

It should be noted that the global situation in respect to electricity generation is very confusing. Instead of closing nuclear plants by 2030, the 2023 Qatar Energy Conference resulted in a call to triple nuclear electricity generation by 2050 [27]. Power plants using fossil fuels were planned to stop work by 2030, but their operation was prolonged by 2050, under some modifications for lower pollution. Progress of renewable sources is undoubtable, under maximum possible capacity.

It is very important to know the equivalent of fossil fuels regarding 1 toe = 1616 kg coal = 1069 m^3 natural gas = 954 kg gasoline = 11.63 MWh = 41.868 GJ (1 kWh = 3.6 MJ). The total annual pollution with CO_2 from fossil fuels at global level stands at 34 Gt, where coal accounts for 45%, oil - 35%, and natural gas - 20% [23], [24], [25], [26], [27], [28]. Electricity generation is responsible for 42.5% of CO_2 emissions in the world, of which 73% belong to coal, with an average value of 950 gCO_2/kWh. (The appropriate value for natural gas is 350g CO_2/kWh).

2024 energy needs in the Republic of North Macedonia are estimated at approx. 2750 ktoe. Final consumption is forecasted at approx. 2075 ktoe [29], [30]. Oil derivatives as energy source account for 43%, followed by coal - 30%, gas - 10%, biomass - 9%, hydropower - 4%, solar - 2.5%, wind - 0.3%, geothermal - 0.2%, and other - 1%. Electricity generation is estimated to cover 26.2% of total energy needs. Gross domestic electricity generation covers 90.2% of gross domestic consumption; with coal (lignite) being the dominant energy fuel - 99.7% [30]. Distribution of the total electricity generation per energy source is as follows: 53% - thermal power plants (coal and oil), 23% - hydropower plants, 16% - natural gas (co-generation TE-TO), 7.8% - renewable sources (approx. 350 ktoe, i.e. 45% by mini and micro hydropower plants, 22% by wind, 18% by solar, and 15% by biogas) [26] [30]. It is easily concluded that consumption of oil products is dominant.

1) Fossil Fuel Sources (Oil, Coal, Gas)

The three basic fossil fuels are coal, oil and gas. The Republic of North Macedonia has only coal, i.e. low-quality lignite with average calorific value of 5500 kJ/kg). Oil and gas are fully imported from different routes and with difficulty. There are two coal-fueled power plants: REK Bitola (675 MW) and REK Oslomej (125 MW), with total installed power of 800 MW, both constructed in the early 1980s with parts manufactured in the former Soviet Union and Poland. TEC Negotino is an oil-fueled power plant with installed power of 195 MW and the oldest plant, dating back at the end of 1970s, also a production of the former Soviet Union. A more recently opened plant (2020) is the gas-fueled co-generation facility (electricity and heating) TE-TO in Skopje, with installed power of 150 MW, but unfortunately it is not in regular work.

All electric machines are synchronous generators, with high speed 3000 1/min for 50 Hz.

Application of power electronics in these power plants is very poor. While being the oldest, TEC Negotino has ASEA automatic voltage regulation (AVR) for excitation. There are no variable speed drives (VSD) for self-used drives – pumps, compressors, fans, transport bands, etc.

TE-TO uses the newest technology available, but is not in regular operation due to occasional lack of gas supply and no thermal energy consumers in summer.

2) Hydro Power Sources (Large, Mini and Micro HPPs)

Hydro sources were the first electricity sources in the Republic of North Macedonia since the beginning of the 20th century. Nowadays, these can be classified as: large (>10 MW), mini (1-10 MW), and micro (<1 MW). The total installed power of large HPPs is 634.4 MW. The total installed power of mini HPPs is estimated at approx. 100 MW. The total installed power of micro HPPs is estimated at approx. 30 MW. Equipment at large HPPs has been largely produced by former Yugoslav manufacturers. Electric machines used are low speed synchronous generators. There is only negligible application of power electronics.

Equipment at mini and micro HPPs is different and variable.

3) Renewable Power Sources

This group includes mini and micro hydro power sources, wind and photovoltaic power sources. It should be noted that the Republic of North Macedonia maintains its top-ranking place among the Western Balkans in terms of energy transition regarding use of renewable sources [31], [32].

4) Wind Power Sources

Key wind power installations in the country include the wind parks in Bogdanci (16x2.3=36.8 MW) and Bogoslovec (8x4.5=36 MW).

The wind park in Bogdanci consists of 16 turbines (Siemens SWT - 2.3 MW - 93 m), which drive induction generators (2200 kW, 1500 rpm, 690 V), speed control range (600 – 1800 rpm), and utilize modular multilevel converters operating in grid-feeding mode.

The wind park in Bogoslovec features double-fed induction generators (4.5 MW, 690 V, 50/60 Hz), manufactured by *Siemens Gamesa*. Power converters linked to the rotor are back-to-back converters rated at 30% of nominal output power.

5) Photovoltaic Power Sources

On the account of its geolocation and climate conditions, the Republic of North Macedonia has around 280 sunny days per year, with an average daily radiation of 3.4-4.2 kWh/m2. The field of solar energy is very dynamic, with the situation changing very fast. It could be estimated that currently more than 400 MW in use come from photovoltaic sources [31], [32]. Dominant installations are connected to the electricity grid, with minor battery use, multi MPPT string, and grid-supporting power inverters.

Example 1 concerns the biggest solar power plant in the Western Balkans, located in Novaci, near REK Bitola, with 3 blocks, equal to a total 675 MW coal-fueled power plant.

Example 1: Solar Power Plant in Novaci [32]

With installed power of 55 MW, this plant was built over a period of ten months by *Mey Energy* and started operation in September 2023. Its investment price amounted to EUR 40 mil. and lifespan of 25 years. The solar plant stretches over 57 ha of land (570,000 m^2), with 101,000 panels (544.55 W/panel) and 856 km of cables, and is connected to the 110 kV grid. Annual electricity generation is estimated at 85 GWh. Figure 1 shows a photo of the solar power plant in Novaci.

Fig. 1. Solar power plant Novaci

6) Biogas Power Sources

To present, there are only 5 facilities using biogas for electricity generation with total installed power of 12 MW ((3+3+3+2+1) MW), relying mainly on chicken waste.

B. Electricity Consumption

The Republic of North Macedonia has the second lowest per capita energy consumption in Europe, which is more than two times lower than EU average. The country's per capita energy consumption in 2022 stood at 1.3 toe (which is by 58% lower than the EU average), including 3200 kWh of electricity (44% lower than the EU average) [23]. The situation in terms of electricity consumption is very similar. ESM (Power Plants of North Macedonia), a state-owned company, accounts for around 2/3 of total electricity generation [24], [25], [26], [27].

Final energy consumption is mainly distributed across four sectors: transport - 35%, households - 27%, industry - 25%, commercial, business and services - 10%. The agricultural sector accounts for consumption of only 1% of energy [29]. Electricity consumption is mainly driven by households, industry and commercial, business and

services [29], [30]. A very important remark in this regard is that the industry practically works at very low capacity.

It is worth saying that in the Republic of North Macedonia oil derivatives are necessary for traffic with internal combustion engines. In reality, there are not enough electricity sources for fast transfer to electric vehicles over a short period of time, because the installed power of vehicles is approx. ten times higher than the installed power of electricity sources. Globally, plans are in place to replace use of internal combustion engines by 2030, but this deadline was prolonged to 2035. Be that as it may, the situation remains unclear and would heavily depend on worldwide policy and wars, including in Europe.

It should be noted that in June 2023 and for the first time, the Republic of North Macedonia noted its peak of electricity consumption in summer. It further justifies the fact that nowadays households and other buildings are the biggest consumers.

1) Industry

Overall, industry in the Republic of North Macedonia is mainly "dirty", with a plethora of metal mines and adequate smelting and other auxiliary capacities. There are two iron mines (Tajmiste and Damjan) and steel work in Skopje, with 5 reduction furnaces (20 MVA each), 1 arc furnace (60 MVA, 120 t) and more rolling mills, hot and cold, with total installed power above 50 MVA, including other auxiliary lines for galvanizing (zinc covering), plasticizing, and strip cutting. At the moment, all these plants are privately-owned and not in regular operation. Furthermore, three lead-zinc mines (Zletovo, Makedonska Kamenica and Toranica) and a smelter are located in Veles, also privately-owned and not in operation. One nickel mine with a smelter are present in Kavadarci, currently not in operation. The chromium mine and accompanying smelter in Jegunovce and its vicinity is not in operation as well. Another mine and smelter (copper, in Radovis) is out of operation as well. While many of the above-listed plants are not in regular operation, main foreign exchange flows in the country come exactly from these industries.

Domestic electricity generation is not sufficient to maintain operation of all these plants at the same time, necessitating electricity import to ensure regular operation.

Equipment and technology applied at these plants date back from the 1970s. VSD mainly use DC motors. Application of VSD with AC motors is in its early stages.

Before the transition, the metal industry (MZT Skopje) was the leading industry in the region, but has nowadays fallen out of use.

The electronics industry is also out of work (EMO - Ohrid, Rade Koncar - Skopje, Cable Factory – Negotino, etc.).

Once a leader in the region, the organic chemical industry (OHIS - Skopje), is currently decommissioned.

The textile industry is plagued by a deep crisis. Back in 1976, GEC Technology in Skopje started work with AC VSD for production of artificial fiber and was among the first in the world, but nowadays it is not in operation. Only a handful of factories across different towns (Stip, Tetovo, Veles, Bitola, Ohrid, Struga, Skopje, etc.) are currently in in regular operation.

Being an agricultural country, the Republic of North Macedonia had great potential for the food processing industry, which dwindled on the account of growing markets in the neighborhood markets and severe competition. A recently emerged trend in this industry with signs of progress concerns small, modern facilities.

Hence, it can be concluded that the industry in the country is in very dire state, often marked by halted production. This has led to the industry loosing its primacy as serious electricity consumer compared to the period before the transition. Moreover, technology applied is already old and obsolete, without any efforts for modernization.

2) Households, Building Needs (HVAC Systems)

Households are a major electricity consumer in the country throughout the year, which is mainly due to use of HVAC systems. Water heating, cooking, washing, home cleaning all heavily rely on electricity consumption as well. Elevators and pumps in multistorey buildings also need electricity.

3) Communal Water Systems

The Republic of North Macedonia has relatively good water sources, with 3 natural lakes (Ohrid, Prespa and Dojran) and many rivers and artificial lakes. However, many towns across the country (Tetovo, Struga, Veles, Prilep, Kumanovo, Berovo, etc.) lack good communal water systems. Water pipelines are old, with only minor application of power electronics and modern drives. It is worth saying that there are more (approx. 10) great water pump stations for water supply in agriculture. Almost all of them use HV 6 kV induction motors, which was considered very advanced at the time of their installation 40-50 years ago, but are currently in bad condition and out of operation.

4) Water Treatment Plants

In the Republic of North Macedonia, water treatment plants are mainly in the stage of planning. Actually, the only operational water treatment plant is located in Kumanovo. Hence, this field opens great possibilities for application of power electronics and modern drives.

5) Transport

Transport in the Republic of North Macedonia almost exclusively uses internal combustion engines. According to most recent statistics [28], the number of passenger vehicles accounts for 477,820, trucks – 44,400, buses – 2,900, and the number of towing vehicles is 6,300, with total population of 1,836,713 (559,418 households). On average, the age of passenger vehicles stands at 19.5 years, 88% of which are older than 10 years. In 2018, the total consumption of diesel accounted for 535,000 t and total consumption of petrol stood at 120,000 t. It could be approximated that the total installed power of vehicles is cca 30000 MW, i.e. 10 times more than the installed power of electricity sources. Moreover, use of 1l of diesel creates 2.68 kg CO_2. All this allows the conclusion that transport is the main reason for air pollution. Trolleybuses, trams, subways, electric buses, etc. are not used for public transport.

The next example presents a case for implementation of electric buses for public transport in Skopje in an attempt to decrease air pollution.

Example 2: Concept of Dynamic Charging System for Public Transport in Skopje [34]

The Public Transport Company Skopje - JSP operates more than 50 urban and 50 suburban bus lines, making it the biggest passenger carrier in the country. The company's bus park is mostly comprised of double-deckers (Yutong, China) and LAZ models from Ukraine, but in much lower numbers. Consequently, the City of Skopje attempted several plans for introduction of tram transport, but with no success. Against the background of global warming and air pollution, the most reasonable and cheap solution to the problem of gas emissions is seen in dynamic charged electric busses. Moreover, a number of city boulevards are facing rush hour congestion, with Blvd Partizanski Ordredi being the most affected by high intensity traffic throughout the entire day. A total of 14 bus lines are operated along this boulevard at all hours, connecting the downtown area with other urban and suburban areas. Use of electric charged buses as part of the In Motion Charging (IMC) system is a possibility for this boulevard, having in mind the multiple lines to be operated and taking into consideration construction of overhead contact line along the boulevard. If constructed, such infrastructure can be used by many vehicles, reducing unit cost (per vehicle or per transport load) of construction and maintenance. The trolleybus route and vehicle charging network suggested as part of the IMC system is shown in Figure 2. Also, Table 5 provides an overview of existing bus lines that use dynamic charging. The trolleybus overhead traction line is 3.5 km long.

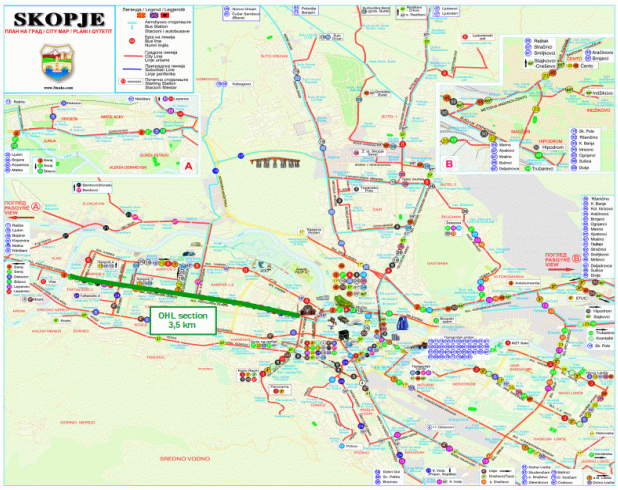

Fig. 2. IMC concept system in Skopje, based on www.jsp.com.mk

While boasting the first line in the Balkans, Thessaloniki-Skopje, constructed in 1873, the railways are in deep crisis. Plans are in place for an east-west connection (Bulgaria-Albania) and a fast line to Serbia, as part of the Budapest-Athens route. The number of hybrid and electric cars in use is negligible, opening great possibilities for power electronics and modern drives in public and private transport. Both public transport projects (modern railway and city electric transport) are given high priority and have great potential to decrease air pollution.

TABLE V
JSP BUS ROUTES PREDESTINED BY IMC OPERATION

Bus route	Route length [km]	Length of route under OHL [km]	Covering of route by OHL
2	13.5	3.5	0.26
2A	14.6	3.5	0.24
4	9.1	3.5	0.38
12	14	3.5	0.25
15	10	2.5	0.25
21	12.5	3.5	0.28
22	12	3.5	0.29
22A	11	3.5	0.32
26	8	2.5	0.31

6) Additional Consumers

As electricity consumers and pollution generators, civil engineering companies are another group that should be noted. In this regard, the main possibility for decreasing pollution is the use of modern technologies.

V. CONCLUSION

Environmental pollution is unavoidable. Unfortunately, the human kind does not demonstrate sufficient care for nature and its own health. However, continuation of life on planet Earth necessitates environmental pollution to be put under control. More especially, environmental air pollution above limits is dangerous for human health and life expectancy. The most important consequences of environmental pollution include climate change and global warming. Human activities are the reasons behind environmental pollution. Even in developed countries, pollution sources do not fully and equitably comply with protection rules. On the other hand, environmental conditions in underdeveloped countries are much dire, including inadequate public and domestic heating systems, use of old buses and cars, low levels of culture and standard, etc. As a developing country and more than 30 years of transition experience, the Republic of North Macedonia faces both the problem of environmental pollution and low application of power electronics. Use of power electronics in electricity generation from renewable sources, modernization of industrial and domestic electric drives, as well as electric transport, can significantly contribute to decrease environmental pollution, even by 50%. It is clear that investments, mainly foreign, are needed, but human health is the most important and has no price tag attached. Such investments usually have a 3 to 5 years rate of recovery, depending on annual operation hours of plants.

REFERENCES

[1] B. K. Bose. "Global Warming: Energy, Environmental Pollution, and the Impact of Power Electronics". IEEE Ind. Electron. Mag., vol.4, no.1, pp. 6–17, March 2010. DOI: 10.1109/MIE.2010.935860.

[2] B. K. Bose. "Power Electronics, Smart Grid, and Renewable Energy Systems". Proc. IEEE, vol.105, no. 11, pp. 2011–2018, November 2017. DOI:10.1109/JPROC.2017.2745621.

[3] Z. Tang, Y, Yang, and F. Blaabjerg. "Power Electronics: The Enabling Technology for Renewable Energy Integration". CSEE J. Power Energy Syst., vol.8, no.1, pp. 39–52, January 2022. DOI:10.17775/CSEEJPES.2021.02850.

[4] J. Rodriguez, F. Blaabjerg, M. P. Kazmierkowski. "Energy Transition Technology: The Role of Power Electronics". vol.111, no.4, April 2023 | PROCEEDINGS OF THE IEEE 329, DOI 10.1109/JPROC.2023.3257421

[5] EU Motor Challenge Program 2008-12, http://energyefficiency.jrc.cec.eu.int

[6] https://www.iqair.com

[7] B. Bose. "Energy, Global Warming and Impact of Power Electronics in the Present Century", chapter in the book *Power Electronics for Renewable Energy Systems, Transportation and Industrial Applications*, ed. by H. Abu-Rub, M. Malinowski. Wiley-IEEE Press, 2014.

[8] D. Ban, D. Zarko, M. Madjercic, Z. Culig, M. Petrinic, B. Tomicic, J. Studir. "Generator Technology for Wind Turbines, Trends in Application and Production in Croatia" (invited paper). 5-th Conference of Mako CIGRE, Ohrid, Macedonia, October 7-9, 2007.

[9] D. Ban, D. Zarko, S Mirchevski. "State of the Art and Tendency for Increased Power Efficiency of Electric Machines and Drives". 6-th Conference of Mako CIGRE, Ohrid, Macedonia, October 4-6, 2009.

[10] S. Mirchevski. "Energy Efficiency in Electric Drives" (invited paper P-4.1). 16th International Symposium on Power Electronics Ee 2011, Novi Sad, Republic of Serbia, October 26- 28, 2011.

[11] "International Energy Agency", (2009) [Online]. Available at: http://www.iea.org

[12] S. Rahman and A. D. Castro. "Environmental Impacts of Electricity Generation: A Global Perspective". IEEE Trans. Energy Conversion, vol.10, pp. 307–313. June, 1995.

[13] G. R. Davis. "Energy for Planet Earth". Sci. Amer., vol.263, no.3, pp. 54–62. Sept. 1990.

[14] U.EPA (2009): http://www.epa.gov/climatechange/

[15] B. K. Bose. "Energy, Environment and Importance of Power Electronics" in proc. IEEE Powering Conf., Setubal, Portugal, April 2007.

[16] B. K. Bose. "Global Warming—How Power Electronics Can Help Solving the Problem", in proc. of 4th IEEE Conf. on Industrial Electronics and Applications, Xi'an, China. May 26, 2009.

[17] B. K. Bose. "Energy, Global Warming and Power Electronics", in proc. 19th Australian Universities Power Engineering Conf. (AUPEC), Adelaide, Australia. September 28, 2009.

[18] B. K. Bose. "Power Electronics and Motor Drives—Recent Progress and Perspective". IEEE Trans. Ind. Electron., vol.56, pp. 1–9. February 2009.

[19] T. Fukao. "Energy, Environment and Power Electronics", pp. 56-68 in Int. Power Electronic Conf. Rec., Japan. April 2005.

[20] J. M. Carrasco, L. G. Franquelo, J. T. Bialasiewicz, E. Galvan, R. C. P. Guisado, A. M. Prats, J. I. Leon, and N. M. Alfonso. "Power-Electronic Systems for the Grid Integration of Renewable Energy Sources: A Survey". IEEE Trans. Ind. Electron., vol.53, pp. 1002–1016. August 2006.

[21] N. Ivkovic. "An Analysis of Electrical Vehicles Impact on the Environmental Pollution" (in Serbian). Journal of Road and Traffic Engineering (43-50), LXVIII, 1/2022

[22] S. Mirchevski, G. Rafajlovski, D. Vidanovski. "How to Improve Operation of Coal Power Plant?". 22nd International Symposium on Power Electronics–Ee 2023, Novi Sad, Serbia.

[23] https://www.consilium.europa.eu/en/infographics/how-is-eu-electricity-produced-and-sold/#:~:text=A%20sunburst%20chart%20showing%20the,Gas%3A19.6%25

[24] https://www.enerdata.net/estore/country-profiles/north-macedonia.html

[25] Energy Development Strategy of the Republic of North Macedonia (final draft for public consultations). MANU, 2019.

[26] 3rd Biennial Update Report on Climate Changes, RNM Ministry of Environment and Spatial Planning, August 2020.

[27] World Summit for Environmental Pollution and Global Warming, Qatar, 2023.

[28] Census of the Republic of North Macedonia, 2021.

[29] https://economy.gov.mk

[30] Reports of RNM State Statistical Office

[31] https://solareyesinternational.com

[32] https://balkangreenenergynews.com

[33] Monthly Reports for Air Pollution in Towns of NM

[34] M. Bartłomiejczyk, M. Połom, K. Jakimovska, L. Jarzębowicz. "Economic Benefits of Dynamic Charging of Electric Buses". Transport for Today's Society Conference, Bitola, 2021.

[35] A.K. Mateska, V. Borozan, P. Krstevski, R. Taleski, S. Borozan, "Gap Analyses between the Legislative Framework of the Electricity Sector in the Republic of North Macedonia and the European Legislation". Journal of Electrical Engineering and Information Technologies, vol.8, no.2 (2023).

[36] M.C. Krsteska, V. Stoilkov, V. Dimchev. "Viability and Performance Investigation of Small Wind Turbines". Journal of Electrical Engineering and Information Technologies, vol.8, no.2 (2023).

[37] M. Srbinovska. "Evaluating the Effectiveness of Meteorological Measurements in Assessing Air Pollution in the Republic of North Macedonia". Journal of Electrical Engineering and Information Technologies, vol.8, no.1 (2023).

[38] M. Srbinovska, V. Andova and M.C. Krsteska. "Assessing the Impact of Air Pollution in North Macedonia: A Meteorological and Green Infrastructure Study". 18th Conference on Sustainable Development of Energy, Water and Environment Systems, Dubrovnik, Croatia. September 24-29, 2023.

[39] M. Srbinovska, V. Andova and M.C. Krsteska, "Breathing Easy in North Macedonia: The Effect of Green Infrastructure and Movement Restrictions on the Air Quality". Future of Digital Society in the Age of AI and ChatGPT, IT IS, Ljubljana, Slovenia (2023).

Journal of Electrical Engineering and Information Technologies, Vol. **9**, No. 2 pp. 100-107 (2024)
Article 224
Received: November 15, 2024
Accepted: November 22, 2024
In print: ISSN 2545–4250
Online: ISSN 2545–4269
UDC: 004.738.5-049.7:621.398]:004.722.4
doi.org/10.51466/JEEIT2492224100s

Original Scientific Paper

COMPARISON OF LORAWAN AND MOBILE IOT NETWORKS AND SERVICES

Hristijan Slavkoski[1)] Toni Janevski

Ss. Cyril and Methodius University in Skopje, Faculty of Electrical Engineering and Information Technologies
1000 Skopje, Macedonia

[1)] hristijanslavkoski@gmail.com

Abstract: The Internet of Things (IoT) is transforming the telecom world by introducing billions of low power devices each day since the start decade of this century. Massive IoT deployments are provided by using mobile IoT technologies in 4G, 5G and beyond. On the other side, there are widespread non-cellular or non-mobile IoT solutions such as LoRaWAN that provide long-range, low-power solution in areas with limited mobile coverage. As more low power and low demanding IoT devices connect to the global Internet, choosing the right network technology for their connectivity is becoming increasingly important. Thus, this paper compares LoRaWAN, used for wide-area networks connecting low power devices, and mobile IoT technologies like Narrowband IoT (NB-IoT) and LTE-M. We compare how these technologies handle data, their battery life, how fast they send data, how many devices they can support, how much data they can handle, and how far their network can reach. This paper contributes to being able to decide which technology is best for different IoT scenarios.

Keywords: 5G networks, Internet of Things, IoT, latency, long range, LoRa, LoRaWAN, LTE-M, NB-IoT, network coverage, QoS, scalability.

СПОРЕДБА НА LORAWAN И МОБИЛНИ IOT МРЕЖИ И УСЛУГИ

Апстракт: Интернетот на нештата (IoT) го трансформира светот на телекомуникациите со воведување милијарди уреди со мала моќност секој ден од почетокот на деценијата на овој век. Масовните распоредувања на IoT се обезбедени со користење на мобилни технологии на IoT во 4G, 5G и пошироко. Од друга страна, постојат и не-целуларни решенија за IoT кои се широко распространети, како што е LoRaWAN, што обезбедува долгорочно решение со мала моќност во области со ограничена мобилна покриеност. Со оглед на тоа што сè повеќе IoT уреди со мала моќност и ниски барања се поврзуваат на глобалниот Интернет, изборот на вистинската мрежна технологија за нивно поврзување станува сè поважен. Оттука, овој труд го споредува LoRaWAN, кој се користи за мрежно поврзување на IoT уреди со мала моќност на поголеми растојанија, и мобилните IoT технологии како теснопојасниот IoT (NB-IoT) и LTE-M. Гледаме како овие технологии се справуваат со податоците, нивната батерија, колку брзо испраќаат податоци, колку уреди можат да поддржат, колку податоци можат да ракуваат и до каде може да достигне нивната мрежа. Зборуваме и за тоа колку лесно се поставуваат и колку чинат. Овој труд допринесува да може да се одлучи која технологија е најдобра за различни сценарија за IoT.

Клучни зборови: 5G мрежи, Интернет на нештата, IoT, латентност, долг дострел, LoRa, LoRaWAN, LTE-M, NB-IoT, мрежна покриеност, QoS, приспособливост

I. INTRODUCTION TO IOT

THE Internet of Things (IoT) is a technology that enables intelligent sensing and actuation for various objects by exchanging information with a core network. This allows people to remotely manage or monitor the behavior of devices from systems located hundreds of kilometers away using various types of IoT technology. In both academia and industry, IoT-based systems have proliferated over the last few years, providing multiple new applications, such as smart homes, intelligent transportation, smart hospitals, and smart cities [1].

Massive IoT refers to applications that are less latency-sensitive and have relatively low throughput requirements but require a huge volume of low-cost, low-energy consumption devices on a network with excellent coverage [2]. The growing popularity of IoT use cases in domains that rely on connectivity spanning large areas, and the ability to handle a vast number of connections, is driving the demand for massive IoT technologies.

One of the core components of IoT networks is connectivity, provided by various types of wired and wireless (terrestrial and non-terrestrial) communication technologies [2]. Among these, Low-Power Wide-Area

Network (LPWAN) has emerged as the preferred connection option for IoT networks due to its long communication range, low energy consumption, and low cost. LPWAN protocols can provide connectivity for numerous low-power battery-operated devices used in delay-tolerant applications with limited throughput per device.

LPWAN technologies like LoRaWAN, Sigfox, NB-IoT, and LTE-M have their own technical features, business models, and deployment strategies. For instance, NB-IoT and LTE-M, standardized by the 3rd Generation Partnership Project (3GPP), operate on the licensed spectrum, offering high data rates and bandwidth with quality-of-service guarantees, albeit at the cost of higher energy consumption and complexity. In contrast, Sigfox and LoRaWAN operate on the unlicensed spectrum, providing long-range communication with low power consumption, suitable for applications where cost and energy efficiency are critical [1], [3].

In summary, the IoT ecosystem's growth, and diversification of its applications, underscore the importance of robust, scalable, and efficient connectivity solutions. LPWAN technologies play an important role in addressing these needs, enabling the deployment of massive IoT networks that support a wide range of applications and services.

II. LoRaWAN Fundamentals

Standardized by the LoRa Alliance in 2015, LoRaWAN is a transformative IoT technology leveraging LoRa's chirp spread spectrum (CSS) modulation in sub-GHz ISM bands, such as 868 MHz in Europe, 915 MHz in North America, and 433 MHz in Asia [4]. CSS spreads a narrow-band signal over a broader bandwidth, enhancing interference resilience, reducing noise, and securing signals. LoRaWAN enables bidirectional communication with adaptable data rates across six spreading factors (SF7 to SF12), balancing communication range and data rates [4]. This adaptability enhances network robustness but can increase deployment costs due to the need for multiple base stations.

This section explores LoRaWAN's architecture and key technologies, including physical and MAC layers, communication protocols, and data handling mechanisms. It highlights how LoRaWAN ensures efficient power use, robust security, and reliable device connections, making it highly effective for diverse IoT applications.

A. LoRa Physical Layer

Developed by *Semtech* in 2014, the LoRa physical layer employs chirp spread spectrum (CSS) modulation across sub-GHz ISM bands [5]. This technique produces chirp signals that maintain a consistent duration but vary in frequency from f_0 to f_1 over time T. In LoRa, there are two primary types of chirps: the base chirp and modulated chirps. The base chirp begins at a minimum frequency $f_{min} = -\frac{BW}{2}$ and rises to a maximum of $f_{max} = +\frac{BW}{2}$, with BW representing the spreading bandwidth of the signal [5]. Modulated chirps are derivatives of the base chirp, cyclically time-shifted to create distinct patterns essential for encoding different digital inputs.

Chirp signals enable robust communication by encoding symbols identified at the receiver through Fast Fourier Transform (FFT) analysis [5]. This process ensures reliable data transmission, even in challenging environments.

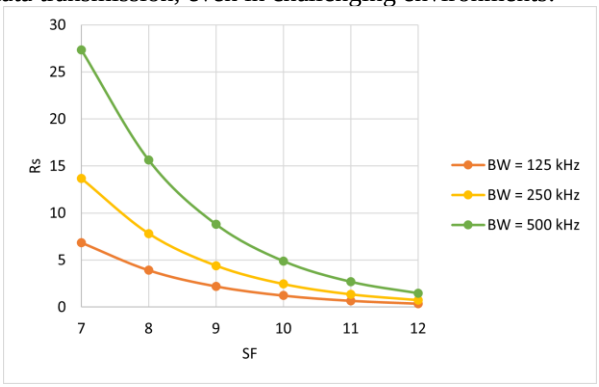

Fig. 1. Variation of the symbol rate *Rs* as a function of spreading factor for different bandwidths

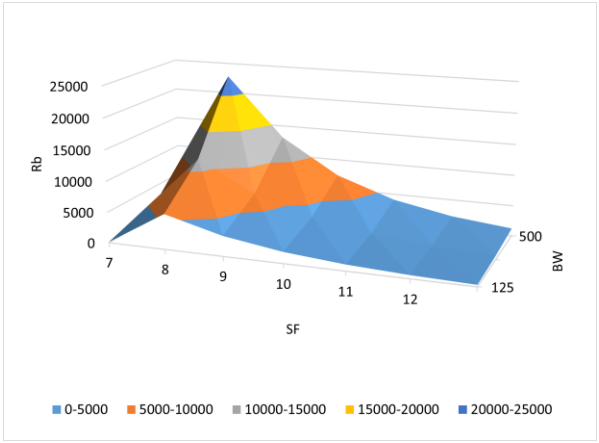

Fig. 2. Data rate Rb as a function of spreading factor and bandwidth for a code rate of 4/5

To describe this process quantitatively, we use two key equations. Equation (1) expresses the symbol rate R_s, where SF is the spreading factor affecting the number of possible cyclic shifts of the base chirp, and BW is the bandwidth in Hz that the signals occupy:

$$R_s = \frac{SF \times BW}{2^{SF}} \tag{1}$$

Equation (2) defines the data rate R_b, incorporating the code rate CR, which adjusts the robustness and error correction capacity:

$$R_b = SF \times \frac{\frac{4}{4+CR}}{\frac{2^{SF}}{BW}} \times 1000 \tag{2}$$

These equations highlight how adjustments in the spreading factor and bandwidth influence the efficiency and capacity of data transmission, essential for maintaining reliable communication across diverse and challenging environments [5].

Following this discussion, Figures 1 and 2 visually demonstrate the relationships outlined in equations (1) and (2), respectively. Figure 1 shows the variation in symbol rate R_s for different bandwidth settings, emphasizing the decrease in R_s with higher SF values. Figure 2 illustrates the impact of similar factors on the data rate R_b for a code rate of 4/5, suggesting similar trends for other code rates (4/6, 4/7 and 4/8).

The LoRa packet structure includes a preamble critical for synchronizing receivers with transmitters. The preamble can extend up to 65,536 symbols, with a fixed sequence followed by a programmable segment to aid in frame detection and synchronization [5]. This design enhances detection accuracy and network reliability, even in diverse operating conditions.

B. LoRaWAN MAC Layer

The MAC layer in LoRaWAN is essential for how devices communicate within the network, sitting above the PHY layer to translate raw data into structured communication between end devices and network infrastructure. It orchestrates complex operations to ensure reliable, efficient, and secure data transmission [6].

A critical function of the MAC layer is managing data rate and network bandwidth through the Adaptive Data Rate (ADR) protocol. ADR dynamically adjusts data transmission settings based on network conditions and device needs, optimizing signal quality and extending battery life [1].

1) Device Classes and Communication Protocols

LoRaWAN devices are categorized into three classes based on network requirements and power availability:

- **Class A**: The most energy-efficient, operates on a schedule allowing two short downlink receive windows after each uplink, suited for minimal downlink communication [1], [7].
- **Class B**: Adds scheduled downlink windows synchronized with gateway beacons to Class A's capabilities, facilitating more predictable communication [1], [7].
- **Class C**: Offers nearly continuous downlink receive windows, ideal for applications requiring low latency communication [1], [7].

2) Network Operations

The LoRaWAN MAC layer employs several protocols and strategies to enhance communication efficiency and ensure network stability:

- **Adaptive Data Rate (ADR)**: ADR optimizes communication settings by adjusting data rate (DR), spreading factor (SF), and transmission power (TP) based on network conditions. In ideal scenarios, it increases DR and reduces SF to conserve battery life by shortening transmission time. Under challenging conditions, ADR increases SF to ensure message delivery, albeit at slower rates. Additionally, ADR modulates transmission power to minimize energy use and network interference for nearby devices, while boosting power for distant ones to maintain stable connections.
- **Joining Procedure and Security**: Secure network access is ensured through two methods: Over-The-Air Activation (OTAA) and Activation by Personalization (ABP). OTAA provides robust security by authenticating devices with the network server during the join process, generating dynamic encryption keys. ABP offers quicker setup by pre-storing static keys, though it is less secure as keys remain unchanged unless updated manually. OTAA is preferred in environments requiring high security, while ABP suits applications where rapid deployment is prioritized.
- **Error Handling and Data Integrity**: Error correction codes and acknowledgment processes are used to detect and rectify data transmission errors, ensuring that messages are accurately received.
- **Channel Management**: The MAC Layer manages channel utilization to avoid collisions and ensure fair bandwidth distribution among all devices. This includes dealing with channel interference and implementing duty cycle restrictions as per regulatory requirements.
- **Downlink Scheduling**: Especially for Class B and Class C devices, the MAC layer schedules downlink transmissions to optimize gateway resources and ensure timely delivery of data without causing network congestion.

This comprehensive approach to network management underscores LoRaWAN's capability to maintain efficient and reliable communication across diverse IoT environments.

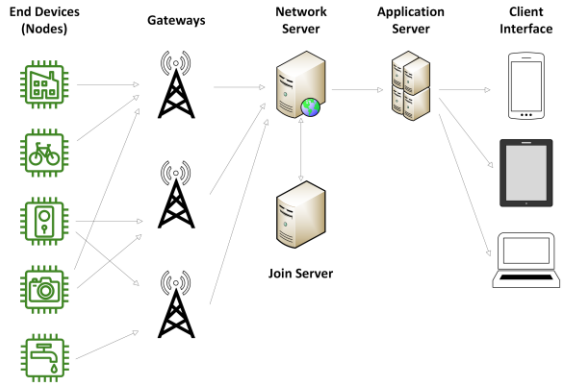

Fig. 3. LoRaWAN topology

C. LoRaWAN Network Topology

The topology of LoRaWAN is a fundamental aspect that enables its widespread application in IoT. It consists of several key components, each playing an essential role in the network's functionality. Understanding the interplay between these elements is very important to appreciate the efficiency and scalability of LoRaWAN. A LoRaWAN network has a star-of-stars topology, as illustrated in Figure 3, and we will explore each component in detail [8].

1) End Devices (Nodes)

End-devices, or nodes, are the 'things' in IoT. They typically comprise a microcontroller, a radio unit, and peripherals like sensors. These nodes use single-hop LoRa communication to transmit data to gateways, boasting low power consumption and extensive range capabilities [8].

2) Gateways

Gateways act as the communication hubs, equipped with LoRa transceivers and baseband processors for decoding multiple channels. They forward messages from nodes to the network server via IP connections like WiFi, Ethernet, or cellular networks, primarily using protocols such as *Semtech*'s UDP and MQTT [8].

3) Server Components

- **Network server:** At the core of the network's architecture, it manages access, routes messages, and handles node authentication and authorization, ensuring efficient message delivery to appropriate LoRaWAN applications [8].

- **Application servers:** Process data from nodes to create downlink payloads for applications, providing essential interfaces for data analysis and management [8].
- **Join server:** Manages over-the-air activation, distributing session keys to ensure secure connectivity within the network [8].

4) Client Interfaces

Client interfaces are the devices through which end-users interact with the system, ranging from mobile phones to desktop computers. They display data and provide interactive controls for managing the IoT environment.

III. LoRaWAN Technologies

While the fundamentals of LoRaWAN provide a solid understanding of its architecture and basic operational mechanisms, the "LoRaWAN Technologies" section delves into the advanced technical enhancements and integrations that expand its applicability and performance in the IoT ecosystem. This section will explore how recent innovations and forward-thinking applications are setting LoRaWAN apart in the competitive landscape of wireless communication technologies.

A. Advanced CSS Modulation Techniques

The LoRa physical layer, introduced in 2014, uses Chirp Spread Spectrum (CSS) modulation to enable long-distance communication while mitigating interference, fading, and Doppler effects. CSS modulates signals into chirp pulses that vary in frequency over time, spreading the signal across a broader bandwidth and reducing noise [1]. Unlike pseudo-random codes used in other spread spectrum techniques, CSS uses base and down-chirps, improving clarity and reach.

The Spreading Factor (SF) determines the number of bits encoded per symbol, ranging from 7 to 12. Higher SF values extend communication range but increase energy usage, while lower values support faster transmission at reduced range. Adjusting transmission parameters, such as bandwidth, coding rate and carrier frequency, further tailor performance based on application requirements. These features, combined with flexible gateway and server configurations, make LoRaWAN suitable for diverse IoT applications [1].

B. Energy Efficiency in LoRaWAN

Energy efficiency is critical for IoT devices in remote or hard-to-reach locations. LoRaWAN excels in this area by using Adaptive Data Rate (ADR) to optimize power usage based on signal quality. For example, ADR adjusts data rates to conserve energy in favorable conditions, extending battery life [8]. Additionally, devices operate in low-power sleep modes, waking only for necessary transmissions, further reducing energy consumption.

Operating on unlicensed frequency bands eliminates spectrum costs, enhancing affordability for businesses and municipalities. These factors, combined with LoRaWAN's long-range capabilities and duty cycling, make it a sustainable choice for IoT systems requiring minimal maintenance and long operational lifespans.

C. Duty Cycling in LoRaWAN

Duty cycling minimizes energy consumption by keeping devices in sleep mode and activating them only when needed. Techniques such as dual SYNC words and distinct uplink/downlink preambles reduce unnecessary energy use by quickly determining message relevance [5]. In dense networks, optimized receive windows and regulatory compliance with duty cycle limits (e.g., 0.1% to 10%) ensure efficient operation while adhering to local guidelines [7].

By balancing energy-saving features with regulatory requirements, duty cycling allows LoRaWAN devices to sustain long-term deployments, even in dense or regulated environments. These mechanisms solidify LoRaWAN as an energy-efficient and cost-effective solution for IoT applications.

IV. Mobile IoT for Telecom Operators (NB-IoT and LTE-M)

As IoT expands, the rollout of 5G networks is transforming connectivity standards, supporting a growing number of devices. Coexisting with 4G, 5G drives innovation in mobile IoT technologies like Narrowband IoT (NB-IoT) and LTE for Machines (LTE-M), which play critical roles in addressing diverse IoT needs, from simple sensor networks to complex industrial systems.

A. Technical Specifications and Advantages of NB-IoT and LTE-M

NB-IoT focuses on low-power, cost-effective communication for distributed devices, offering strong indoor and underground signal penetration. Standardized in 3GPP Release 13, it operates in LTE carriers, guard bands, or standalone mode, using a narrow 180 kHz bandwidth for high spectrum efficiency. Its simplicity keeps costs low, making it suitable for applications like utility metering and agricultural monitoring [9].

LTE-M, also standardized in 3GPP Release 13, supports higher data rates and mobility, with peak speeds up to four times faster than NB-IoT. It is ideal for applications requiring voice support and real-time data, such as health monitoring and vehicle tracking. LTE-M's energy-saving features allow for up to 10 years of battery life, while its compatibility with legacy networks and flexible duplex configurations enhances versatility [9], [10].

Both NB-IoT and LTE-M strengthen cellular networks to meet diverse IoT demands, reflecting strategic advancements in mobile technology.

B. Strategic Role of NB-IoT and LTE-M in Enhancing 5G IoT Connectivity

As 5G networks expand, NB-IoT and LTE-M have become integral to addressing the limitations of earlier network generations. These technologies enable large-scale, energy-efficient connectivity, supporting high device densities and enhancing indoor coverage.

NB-IoT excels in low-data, long-distance applications such as utility metering and agricultural monitoring, while LTE-M supports higher data needs and mobility for use cases like health monitoring and vehicle tracking [10]. Together, they fulfill 5G's goal of connecting diverse IoT environments, from urban centers to remote regions, with reliable and scalable solutions.

As 5G grows, NB-IoT and LTE-M will underpin advanced IoT systems ranging from simple sensors to

complex smart grids and industrial processes, driven by significant investments from mobile operators upgrading infrastructure to meet increasing IoT demands [9], [10].

V. Comparison of LoRaWAN Non-Mobile and IoT Mobile Technologies NB-IoT and LTE-M

As the Internet of Things (IoT) grows, it is important to pick the right technology for different IoT applications. In this section, we will compare three major IoT technologies: LoRaWAN, NB-IoT, and LTE-M. Each one has its own benefits and fits different kinds of IoT setups. We will look at several important factors that you should consider when choosing an IoT technology. These factors include quality of service (QoS), battery life, latency, how many devices it can support, how much data it can send, how far and wide it can cover, how it is set up, and how much it costs. Understanding these points will help decide which technology is best for certain IoT needs, whether they are mobile or fixed. This comparison will clearly show how each technology works in different situations and explain why one might be better than another in certain cases.

A. Quality of Service (QoS)

QoS measures the reliability, data rate, and overall performance of a network, making it crucial for applications requiring consistent and dependable data transfer.

- **LoRaWAN**: LoRaWAN uses chirp spread spectrum (CSS) technology, providing a reliable connection in interference-prone environments. It dynamically adjusts data rates through bandwidth and spreading factor changes based on signal strength and distance. While this adaptability enables stable connections over long ranges, it can limit data rates when operating at extended distances [4].
- **NB-IoT**: By operating on a licensed LTE spectrum and employing synchronous protocols, NB-IoT ensures a stable connection with higher throughput than LoRaWAN. The licensed spectrum minimizes interference, making NB-IoT ideal for critical applications requiring predictable connectivity, such as smart metering and urban IoT deployments [11].
- **LTE-M**: LTE-M shares the licensed spectrum advantage with NB-IoT but supports higher data rates and lower latency, making it suitable for data-intensive and real-time applications like wearable health devices and emergency systems. Its robust QoS is tailored for scenarios where both reliability and responsiveness are vital [12].

In terms of QoS, both LTE-M and NB-IoT outperform LoRaWAN in QoS due to their licensed spectrum and advanced protocols. While LoRaWAN excels in long-range, low-cost deployments with minimal infrastructure, its QoS is less suited for high-data-rate or latency-sensitive applications.

B. Battery Life

Battery life is a critical factor in IoT deployments, especially for devices in remote locations where frequent maintenance is impractical. Each technology employs different strategies to optimize energy efficiency.

- **LoRaWAN**: Renowned for its low power consumption, LoRaWAN uses asynchronous communication, where devices transmit data only when necessary. Following the ALOHA protocol, this minimizes energy use and allows devices like environmental sensors or agricultural monitors to operate for extended periods on a single battery charge [11].
- **NB-IoT**: NB-IoT incorporates power-saving features such as extended Discontinuous Reception (eDRX) and Power Saving Mode (PSM), enabling devices to remain in low-power states for long durations, waking only for scheduled transmissions. While NB-IoT requires more power during active communication due to its synchronous protocol, these features make it ideal for use cases like utility metering and asset tracking, where data is reported intermittently [13], [14].
- **LTE-M**: LTE-M also leverages eDRX and PSM for energy efficiency, allowing devices to balance extended battery life with higher data rates and frequent communication needs. Unlike NB-IoT, LTE-M supports advanced features such as voice over LTE while maintaining efficient power usage, making it suitable for applications requiring both performance and longevity [14].

Each technology offers unique advantages: LoRaWAN excels in ultra-low-power, infrequent transmissions, NB-IoT balances efficiency with reliability for periodic updates, and LTE-M combines battery life with robust performance for versatile applications. Choosing the right technology depends on the device's operational needs and the desired battery longevity.

C. Latency

Latency, the time taken for data to travel from source to destination, is critical for applications requiring real-time or near-real-time data processing.

- **LoRaWAN**: LoRaWAN typically exhibits higher latency due to its asynchronous communication protocol, where devices transmit data only when needed. While this approach conserves battery life, it results in delays that make it unsuitable for real-time applications. Class C devices can reduce latency by continuously listening for data, though at the cost of higher power consumption [4]. LoRaWAN is best suited for use cases like environmental monitoring, where occasional delays are acceptable [15].
- **NB-IoT**: NB-IoT achieves lower latency compared to LoRaWAN by using structured communication protocols over licensed LTE bands. This makes it suitable for applications like emergency alerts and real-time health monitoring, where timely data delivery is crucial. However, the reduced latency comes with higher power consumption, which may impact battery life in devices [4], [15].
- **LTE-M**: LTE-M provides the lowest latency of the three, with response times as low as 50-100 ms. It supports high data rates and real-time communication, making it ideal for demanding applications such as voice services, mobile monitoring systems, and advanced tracking. LTE-M combines low latency with robust performance, catering to both static and mobile IoT environments [15].

In conclusion, LoRaWAN is suitable for non-critical applications prioritizing battery life and wide-area coverage. NB-IoT balances moderate latency with reliable data delivery, fitting well in urban and industrial settings. LTE-M excels in real-time, latency-sensitive scenarios, making it the top choice for high-demand IoT applications like emergency services or mobile tracking.

D. Scalability

Scalability refers to an IoT network's ability to handle increasing device numbers and data volumes without performance degradation.

- **LoRaWAN**: Designed for wide-area, low-data-rate applications, LoRaWAN uses a simple ALOHA protocol that allows devices to transmit data independently, minimizing network coordination overhead [4]. While this approach supports moderate device densities, it may lead to packet collisions in highly dense networks, potentially limiting scalability.
- **NB-IoT**: NB-IoT significantly improves scalability, supporting up to 100,000 devices per cell by leveraging licensed spectrum and LTE-based signaling protocols [13]. Its structured network management ensures reliable performance in dense urban environments, making it ideal for large-scale IoT deployments requiring high connection density and stability.
- **LTE-M**: Similar to NB-IoT, LTE-M offers robust scalability but adds support for higher data throughput and lower latency. This makes LTE-M suitable for data-intensive applications like video surveillance and vehicle telematics, where both large-scale device connectivity and substantial data handling are needed [13].

In summary, LoRaWAN is better suited for moderate-density, low-data-rate applications with wide-area coverage. NB-IoT and LTE-M, with their LTE-based infrastructure, excel in managing high device densities and ensuring performance in urban and industrial IoT scenarios.

E. Payload Length

Payload length determines the type and volume of data that can be transmitted in a single message, making it a critical factor for applications like firmware updates, multimedia, or detailed sensor readings.

- **LoRaWAN**: LoRaWAN supports a maximum payload size of up to 243 bytes per transmission [4], [15]. This is sufficient for most IoT applications that send small data packets, such as temperature readings or GPS coordinates. The smaller payload size helps maintain LoRaWAN's low power usage and long-range capabilities, though it limits suitability for data-heavy use cases.
- **NB-IoT**: NB-IoT offers a significantly larger payload capacity of up to 1600 bytes [4], [15]. This makes it ideal for applications requiring substantial data transmission, such as utility metering or remote configuration of devices. The higher payload size provides flexibility for data-intensive applications.
- **LTE-M**: LTE-M supports a maximum payload size of 1000 bytes [15], striking a balance between NB-IoT and LoRaWAN. This capacity enables LTE-M to handle moderate data-intensive applications, such as voice over LTE (VoLTE) or aggregated sensor data, while maintaining energy efficiency.

LoRaWAN shines in scenarios requiring minimal data transmission over wide areas with low power consumption. NB-IoT is well-suited for data-intensive applications where power efficiency is less critical. LTE-M strikes a balance between the two, offering efficient performance for moderate data needs and versatile applications.

F. Network Coverage and Range

Coverage and range are key factors in IoT technology selection, determining network accessibility across various environments and the density of required base stations.

- **LoRaWAN**: LoRaWAN provides extensive coverage, with a single gateway covering up to 5 km in urban areas and up to 20 km in rural settings, depending on the environment and placement [15]. This makes it ideal for applications like remote monitoring and agriculture, where devices are spread across wide areas with minimal infrastructure.
- **NB-IoT**: Operating within the LTE framework, NB-IoT offers a shorter range compared to LoRaWAN, typically up to 10 km in rural areas and around 1 km in urban environments [15]. Its reliance on cellular infrastructure enables strong in-building penetration, making it suitable for urban applications like smart meters and indoor tracking. However, its range limitations may pose challenges in rural or remote areas without LTE infrastructure.
- **LTE-M**: LTE-M provides similar coverage to NB-IoT, with ranges exceeding 5 km depending on deployment specifics. Its ability to maintain signal integrity at high speeds and handle higher data rates makes it well-suited for mobile applications like vehicle tracking and emergency services [15].

LoRaWAN's extensive range and low base station density make it ideal for wide-area deployments like agriculture and remote monitoring. NB-IoT, with its strong in-building penetration and reliance on LTE infrastructure, is a reliable choice for urban and indoor applications. LTE-M bridges the gap by combining mobility support with robust coverage, offering flexibility for diverse IoT use cases such as vehicle tracking and emergency services.

G. Deployment Models

IoT technologies vary in their deployment models, influenced by flexibility, infrastructure requirements, and geographical suitability [13].

- **LoRaWAN**: LoRaWAN offers flexible deployment options, functioning as a private local network or a public network. Its hybrid model allows simultaneous coverage of localized operations, like factory floors, and broader regional areas with minimal infrastructure. This adaptability makes it ideal for varied applications requiring extensive geographic coverage and cost efficiency [4], [13].
- **NB-IoT**: Integrated into existing cellular networks, NB-IoT relies on licensed spectrum bands, enabling rapid deployment in urban areas with robust LTE infrastructure [13]. However, its reliance on cellular networks limits deployment flexibility in rural or underdeveloped regions. NB-IoT excels in providing

reliable, deep indoor coverage in dense urban environments.

- **LTE-M**: LTE-M builds on the cellular infrastructure of NB-IoT but adds support for mobility and higher data rates [13]. This makes it suitable for applications like asset tracking and emergency services, where reliable coverage and mobility are critical. LTE-M benefits from established cellular networks, ensuring robust performance for a wide range of mobile and stationary IoT deployments.

Each technology caters to specific needs: **LoRaWAN** is best for flexible, cost-efficient deployments across wide areas, while **NB-IoT** and **LTE-M** leverage cellular infrastructure to provide reliable coverage in urban and industrial settings. LTE-M's mobility support further broadens its application scope, making it the preferred choice for use cases requiring both coverage and mobility.

H. Cost Considerations

Cost is a key factor when selecting IoT technologies, with deployment costs varying based on infrastructure needs and spectrum usage.

- **LoRaWAN**: LoRaWAN is the most cost-effective option for wide-area, low-density applications. Its use of unlicensed spectrum eliminates spectrum fees, and its ability to cover large areas with fewer base stations reduces infrastructure costs. This makes it ideal for agricultural monitoring or remote asset tracking [13].
- **NB-IoT**: NB-IoT involves higher costs due to its reliance on licensed spectrum and existing cellular infrastructure [13]. Deployment can be expensive in areas lacking LTE coverage but is cost-effective in urban settings with dense device deployments, where its reliable connectivity and deep penetration justify the expenditure.
- **LTE-M**: LTE-M also operates on licensed spectrum, resulting in higher deployment costs like NB-IoT [13]. However, its support for real-time communication, voice services, and mobility justifies the investment in complex applications like emergency services and vehicle tracking. LTE-M's broad functionality often translates to a higher return on investment in scenarios requiring both data intensity and mobility.

I. Overall Evaluation and Conclusion

In assessing the performance and suitability of LoRaWAN, NB-IoT, and LTE-M across various parameters, it is clear that each technology offers distinct advantages based on specific application needs. Figure 4 provides a visual representation of the summary based on previous discussion.

Each IoT technology has its optimal use cases based on its unique strengths. LoRaWAN is best suited for applications requiring broad coverage with minimal data transmission, making it ideal for agricultural or environmental monitoring in remote areas. NB-IoT excels in urban environments where high reliability is needed, such as for smart city applications and indoor monitoring. LTE-M, with its higher data rates and lower latency, is perfect for mobile applications and services that demand real-time communication, such as emergency services or vehicle tracking. The choice of technology should align with the specific requirements of coverage, data needs, and operational environment.

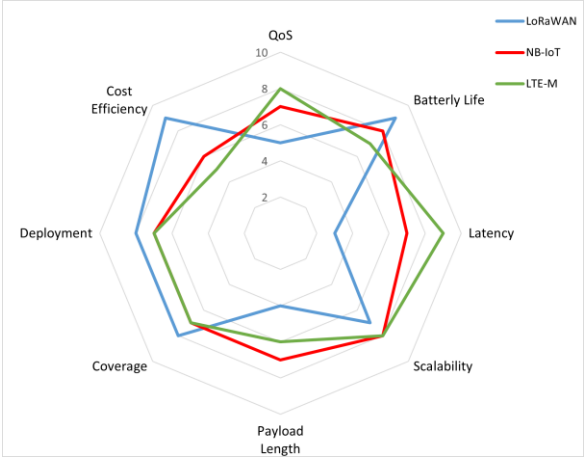

Fig. 4. LoRaWAN, NB-IoT and LTE-M main characteristics

VI. Telecommunication Business and Regulatory Aspects for IoT Including LoRaWAN

The 5G technology is a big change in the Internet of Things (IoT) landscape, affecting how businesses in telecommunications operate and how they are regulated. 5G is more than just a step up from previous technologies; it is a complete system designed to improve and bring together different IoT technologies. This system includes things like radio access technologies, network setups, cloud services, and devices that customers use, all managed by mobile network operators and service providers.

5G supports a massive number of connected devices, creating new opportunities across industries like healthcare, manufacturing, and smart cities. However, it also presents challenges related to regulatory compliance, network security, and data privacy. Organizations must navigate complex rules while ensuring robust security frameworks to support IoT deployments. Additionally, 5G complements technologies like LoRaWAN, which operates in unlicensed bands, by enabling hybrid connectivity models. This integration demonstrates 5G's potential to unify various IoT networks, fostering a more connected world.

A. Strategic IoT Approaches for Telecom Operators in the 5G Era

In the 5G era, telecom operators are well-positioned to lead the IoT revolution, thanks to their extensive network infrastructure and long-standing presence in the market Their established trust with customers helps smooth the adoption of IoT services, as people are more likely to accept new technologies from familiar providers [16], [17].

Over the years, operators have developed robust ecosystems, including physical infrastructure, customer support, and device management, allowing them to manage IoT services cost-effectively. Their expertise in network security and handling large-scale connectivity also ensures secure and efficient IoT deployments [16].

As 5G evolves, telecom operators are enhancing their networks to meet growing IoT demands, supporting applications like smart cities, health monitoring, and

industrial automation. These advancements pave the way for new business models and opportunities in the IoT space.

B. Regulatory Considerations and Business Models in IoT Deployment

IoT technologies operate under varying rules and business models, influencing their deployment and accessibility. For instance, NB-IoT operates on licensed frequency bands, meaning only mobile network operators with a 4G license can offer NB-IoT services. This model allows operators to leverage existing infrastructure, minimizing legal hurdles and enabling quick deployment in many regions. However, because these services are tied to operators, they come with subscription costs for users. LTE-M, similar to NB-IoT, operates on licensed bands and offers higher data rates and voice support, making it suitable for a wider range of applications. Nevertheless, LTE-M shares similar regulatory constraints and cost implications, as it remains tied to operator-controlled deployment and pricing [3].

On the other hand, LoRaWAN uses unlicensed spectrum, allowing anyone to set up a network without requiring spectrum licensing. This flexibility reduces regulatory barriers, making LoRaWAN an attractive option for community-driven networks, such as The Things Network. In Europe, guidelines like CEPT Recommendation 70-03 govern LoRaWAN's use, but interpretations vary between countries. While this can make LoRaWAN easier and cheaper to deploy, it can also lead to inconsistencies in service and coverage due to the lack of unified standard [3].

While NB-IoT and LTE-M offer reliability and structured deployment through licensed networks, LoRaWAN provides flexibility and cost-efficiency by operating in unlicensed bands. The choice of technology depends on balancing regulatory ease, deployment costs, and specific application needs.

VII. CONCLUSIONS

In recent years, the Internet of Things (IoT) has seen remarkable growth, revolutionizing how we connect and manage devices across various sectors. This rise has been significantly supported by evolving technologies like LoRaWAN, NB-IoT, and LTE-M, each bringing unique strengths to the table, tailored to different application needs. When choosing the right technology for an IoT project, it is essential to consider the specific requirements of the task at hand, as there no a one-size-fits-all solution.

LoRaWAN stands out for its wide coverage and low power requirement, making it ideal for monitoring vast, remote areas such as farms or natural environments. On the other hand, NB-IoT is a better fit for urban settings where reliable connections and the ability to penetrate buildings are important, which is why it is often used in smart city initiatives and indoor applications. Meanwhile, LTE-M caters to scenarios that require mobility and real-time data transmission, such as tracking vehicles or emergency services.

Telecom operators are also playing a key role in advancing IoT through deployed 5G networks, increasing the capabilities and reach of technologies like NB-IoT and LTE-M. These developments are opening up new possibilities for IoT applications, offering better service options and supporting a broader range of business models.

In conclusion, as IoT continues to expand and develop, choosing the appropriate technology is very important and should be based on the unique requirements of each application. There is no inherently superior technology, each has its place based on its strengths. With the ongoing support of telecom operators and continuous improvement of network technologies, the future of IoT looks promising, offering more customized and efficient solutions for a connected world.

REFERENCES

[1] Mohammed Jouhari, Nasir Saeed, Mohamed-Slim Alouini, El Mehdi Amhoud. "A Survey on Scalable LoRaWAN for Massive IoT: Recent Advances, Potentials, and Challenges". IEEE Communications Surveys & Tutorials, vol.25, no.3, 2023.

[2] Claes Lundqvist, Ari Keränen, Ben Smeets, Carlos R. B. Azevedo, John Fornehed, Peter von Wrycza. "Key Technology Choices for Optimal Massive IoT Devices". Ericsson Review, no.12, Sweden, 2018.

[3] Riccardo Marini, Konstantin Mikhaylov, Gianni Pasolini, Chiara Buratti. "Low-Power Wide-Area Networks: Comparison of LoRaWAN and NB-IoT Performance". IEEE Internet of Things Journal, vol.9, no.21, November 2022.

[4] Kais Mekki, Eddy Bajic, Frederic Chaxel, Fernand Meyer. "A Comparative Study of LPWAN Technologies for Large-Scale IoT Deployment". ICT Express, vol.5, France, 2019.

[5] Jetmir Haxhibeqiri, Eli De Poorter, Ingrid Moerman, Jeroen Hoebeke. "A Survey of LoRaWAN for IoT: From Technology to Application". Sensors, vol.18, 3995, 2018.

[6] Mounika Baddula, Biplob Ray, Morshed Chowdhury. "Performance Evaluation of Aloha and CSMA for LoRaWAN Network". 2020 IEEE Asia-Pacific Conference on Computer Science and Data Engineering (CSDE), 2020.

[7] Mohamed Saban, Otman Aghzout, Leandro D. Medus, Alfredo Rosado. "Experimental Analysis of IoT Networks Based on LoRa/LoRaWAN under Indoor and Outdoor Environments: Performance and Limitations". IFAC PapersOnLine, vol.54, no.4, 2021.

[8] Ali Loubany, Samer Lahoud, Abed Ellatif Samhat, Melhem El Helou. "Improving Energy Efficiency in LoRaWAN Networks with Multiple Gateways". Sensors, vol.23, 531515, 2023.

[9] Roberto Verdone, Silvia Mignardi. "IoT Support" in 5G Italy White eBook: From Research to Market, Consorzio Nazionale Interuniversitario per le Telecomunicazioni, Italy 2018.

[10] GSMA, "Internet of Things in the 5G Era: Opportunities and Benefits for Enterprises and Consumers". UK, 2019.

[11] Shilpa Devalal, A. Karthikeyan. "LoRa Technology-An Overview", IEEE Conference Record #42487; IEEE Xplore ISBN: 978-1-5386-0965-1, 2018.

[12] Hamidou Adamou Ismael, Ahmed Laguidi, Youssef Mejdoub. "A Comparative Study on LPWAN Standards: Nb-IoT and LTE-M". ITM Web of Conferences, vol.52, 01007, 2023.

[13] Mohammad Istiak Hossain, Jan I. Markendahl. "Comparison of LPWAN Technologies: Cost Structure and Scalability". School of Electrical Engineering and Computer Science, KTH Royal Institute of Technology, Sweden 2021.

[14] Tanu Goyal, Sakshi Kaushal. "An Intelligent Energy Efficient Handover Mechanism with Adaptive Discontinuous Reception in Next Generation Telecommunication Networks". Thapar Institute of Engineering and Technology; Computer Science and Engineering, UIET, Panjab University, India, 2022.

[15] Ala' Khalifeh, Khaled Aldahdouh, Khalid A. Darabkh, Waleed Al-Sit. "A Survey of 5G Emerging Wireless Technologies Featuring LoRaWAN, Sigfox, NB-IoT and LTE-M". IEEE International Conference on Wireless Communications Signal Processing and Networking (WiSPNET), 2019.

[16] Toni Janevski. "QoS for Fixed and Mobile Ultra-Broadband". Wiley – IEEE Press, 2019.

[17] Toni Janevski. "Future Fixed and Mobile Broadband Internet, Clouds, and IoT/AI". Wiley – IEEE Press,

Journal of Electrical Engineering and Information Technologies, Vol. **9**, No. 2 pp. 108-115 (2024)
Article 225
Received: November 19, 2024
Accepted: November 25, 2024
In print: ISSN 2545–4250
On line: ISSN 2545–4269
UDC: 004.8:621.39]:339.13.025
doi.org/10.51466/JEEIT2492225108t

Original Scientific Pape

SURVEY ON TECHNICAL, BUSINESS AND REGULATORY ASPECTS OF ARTIFICIAL INTELLIGENCE IN TELECOM NETWORKS AND SERVICES

Dimitar Tanevski [1)] Toni Janevski Venceslav Kafedziski

Ss. Cyril and Methodius University in Skopje, Faculty of Electrical Engineering and Information Technologies
1000 Skopje, Macedonia

[1)] dimitartanevski@yahoo.com

Abstract: The advancement of AI/ML models, along with the complexity of new-generation networks, including IMT-2020, has made AI functionality indispensable in telecom architecture and business strategies. Standardization bodies such as ETSI and ITU-T have established the foundation for architectural frameworks, with ITU-T Y.3172 and ETSI's ENI models, leading to various recommendations and supplementary documents covering internal communication, quality of service, fault and recovery, and security frameworks and procedures. Globally, regulatory efforts surrounding AI in telecom, such as the EU's Artificial Intelligence (AI) Act and initiatives from the U.S. and China, emphasize risk categorization, fines for non-compliance, and ethical principles to ensure responsible deployment. Industry collaborations, exemplified by Nokia and NVIDIA's partnership for tech efficiency, and the deployment of AI-driven chatbots by telecom giants like AT&T, Deutsche Telekom, and Vodafone, highlight tangible benefits such as reduced costs, improved performance, and enhanced customer experience. These advancements not only drive down CAPEX and OPEX but also fuel revenue growth and bolster customer satisfaction, underscoring the transformative impact of AI in telecommunications

Keywords: Artificial Intelligence (AI), AI governance, AI regulation, AI standardization, business aspects of AI

ТЕХНИЧКИ, БИЗНИС И РЕГУЛАТОРНИ АСПЕКТИ НА ВЕШТАЧКАТА ИНТЕЛИГЕНЦИЈА ВО ТЕЛЕКОМУНИКАЦИСКИТЕ МРЕЖИ И СЕРВИСИ

Апстракт: Напредокот на AI/ML моделите, паралелно со зголемената комплексност во мрежите од новата генерација, вклучително IMT-2020, ја направија AI функционалноста неразделив дел од телекомуникациската архитектура и бизнис стратегијата. Стандардизационите тела како ETSI и ITU-T ја воспоставија основата за архитектурните рамки, со ITU-T Y.3172 и ETSI ENI моделите, презентирајќи различни препораки и пропратни документи кои покриваат внатрешна комуникација, квалитет на услугата, управување со грешки и безбедносни рамки и процедури. Глобално, регулаторните напори околу AI во телекомуникациите, како што се AI актот на ЕУ и легислативните иницијативи на САД и Кина, нагласуваат категоризација на ризиците, казни за непочитување и етички принципи, обезбедувајќи одговорна имплементација. Индустриските соработки, како што е партнерството меѓу Nokia и NVIDIA за технолошка ефикасност, и имплементацијата на AI-управувани чатботови од телекомуникациски гиганти како AT&T, Deutsche Telekom и Vodafone, истакнуваат конкретни придобивки како намалување на трошоци, подобрени перформанси и подобрено корисничко искуство. Овие напредоци не само што ги намалуваат CAPEX и OPEX, туку го поттикнуваат растот на приходите и го зголемуваат корисничкото задоволство, нагласувајќи го трансформативното влијание на AI во телекомуникациите.

Клучни зборови: ретроспективна дозиметрија, термолуминисценција, оптички стимулирана луминисценција вештачка интелигенција (ВИ), деловни аспекти на ВИ, управување со ВИ, ргулатива за ВИ, стандардизација на ВИ.

I. INTRODUCTION

FUTURE networks face evolving requirements, including increased bandwidth, QoS, personalized services, and heterogeneous access technologies, adding complexity to network management. Efficiently handling these complexities through manual intervention is becoming infeasible. In recent years, AI/ML models have become integral to technological frameworks, with the path to 6G and next-gen networks emphasizing AI alongside traditional network requirements [2]-[4]. The growing complexity of networks and business demands underscore the need for AI/ML to optimize CAPEX and OPEX in deployment, operation, and maintenance. Projections predict a CAGR of 41.4% from 2022 to 2031. A recent *NVIDIA* survey found 56% of telecom companies

see AI as crucial to their success, with 90% actively implementing AI. Notably, 48% are piloting AI, while 41% have integrated it into operations. AI adoption aims to improve customer experience (48%) and reduce costs (35%), with most companies seeing revenue increases and lower operational expenses, yielding ROI within five years.

In 2023, generative AI emerged as a leading model, particularly in chatbots and digital assistants. However, AI implementation comes with challenges, such as shortage of professionals and interoperability issues across telecom network segments. To address these, ITU-T has issued several recommendations. ITU-T Y.3115 provides guidelines for integrating AI into existing networks, while Y.3170 specifies ML-based QoS assurance for IMT-2020 networks [6] [7]. Y.3172 outlines an ML framework for IMT-2020, detailing interfaces and enablers for efficient deployment [8]. Y.3183 focuses on QoE translation into network parameters with AI-driven policies [9], and Y.3177 suggests a framework for AI-based network automation [10].

Parallel efforts by ETSI's ENI ISG define Cognitive Network Management using AI, proposing an architectural framework for personalized services [11]. Recommendations like ENI ETSI 002 outline the requirements for implementing ENI, while ENI ETSI 003 discusses context-aware policies [12] [13]. The ENI group has conducted 22 Proof of Concepts (PoCs) to demonstrate the feasibility of this framework [17].

Implementation of AI/ML models in telecom networks requires extensive data, often involving customer personal data. This data must be handled carefully to avoid privacy breaches and comply with GDPR regulations. Additionally, AI models must be constructed to avoid discrimination or manipulation of consumer behavior. Various countries have introduced legislation to regulate AI use, with the EU having the strictest regulations, followed by China, while the U.S. has more lenient policies.

The structure of this paper is as follows: Section II explores ITU and ETSI architectural frameworks, their components, interfaces, and a Fault and Recovery Model for AI validation. Section III discusses global legislative measures relevant to AI in telecom. Section IV highlights practical AI implementations and business motivations. Section V concludes the paper.

II. AI/ML Architectures

Machine Learning (ML) will be essential tool in every segment of telecommunication networks, giving a way of generalized learning, prediction, optimization and preventive actions such as fault detection and recovery. However, implementation of ML algorithms is a novelty in operations and maintenance procedures for telco ISPs. This poses the question for cost-effective and seamless ways for incorporating ML in networks of the new generation. These algorithms and models are data driven, making it essential to detect the sources of information, connections and resources needed for efficient implementation.

A. ITU-T AI/ML Framework

The new generation networks are introducing a whole new level of heterogeneity, i.e. diversity in the RAN segment (different RAT, devices), linked to diversity in the core network (CN), and possibility for network slicing. In general, challenges brought about with introduction of ML in telco networks are grouped in 4 categories according to ITU-T Y.3172 [8]:

- Coping with the heterogeneous nature of the networks;
- Unified development and roadmap alignment between ML functionalities and networks;
- Finding efficient way for cost-effective and seamless integration in telco network architectures;
- Estimating and minimizing the impact on operations and maintenance procedures of communication networks.

To mitigate disputed points of ML implementation and integration, the ITU-T Y.3172 Recommendation proposes a generalized architectural framework.

The framework defines 5 types of high-level architectural requirements, on the basis of which multiple recommendations for lower-level architectures and functionalities are developed – enablers for data correlation sourced from heterogeneous technologies, enablers for deployment, requirements related to interfaces between different architectural components, requirements for declarative specification of ML applications, and requirements related to management.

The enablers for correlation define a requirement for ML architecture that is able to support correlation between data sets from different sources in the network. This is due to multi-level dependencies of a given parameter linked with different network functions (NFs) deployed in separate segments in the network. A good example of this is the QoS parameter in end-to-end user flows, which is interdependent with performance in the access network (AN) and the core network (CN). Also, ML architecture is required to provide support of different technologies at the same time. This can be illustrated with an example where slices designed for different technologies should coexist and be optimized for providing a required end-to-end QoS. Since multilevel and heterogeneous data is introduced in this section, it is obvious that postprocessing and analysis will be carried in distributed manner. That means that ML architecture should support distributed instantiation of machine learning functionalities and data transfer. Often, data analysis required for CN (core network) is dependent on information gathered in AN (access network), thus preprocessed AN data should be transferred and correlated at CN level.

The enablers for deployment specify the required flexible placement of ML functions, based on defined resource (e.g., computational load, availability of data, dedicated HW) and parameters constraints (e.g., latency, QoS). For instance, ML algorithms perform better in GPU environment than in CPU, so deployment should be flexible enough to meet these requirements regardless of data sources. In addition, a well-known practice for real-time latency applications is to place ML functionalities closer to the edge segment of the network (Edge Cloud Computing).

On top of the aforementioned, ML architecture should

provide dynamic pluggable interfaces for new data sources, based on the requirements for detection. This is especially popular in anomaly detection for mIoT (massive IoT) cases.

Another essential feature is the distinction between model training and model usage. This is introduced through variable interfaces linked to ML functionalities. Certain segments of the network may have the data needed for model training, but they could lack HW resources for such task, and vice versa. The framework suggests flexible training and deployment of trained models, based on the needs and capabilities of the specific network segment. Moreover, this represents a dependency for data exchange between different network segments which, as mentioned above, are the main enabler for data correlation.

Given the plethora of services and vendors building and using the telecommunication network, the framework defines a need for declarative specification for representing ML applications, which could later be translated into a specific set of ML functionalities and parameters enabled by the underlay network architecture. The framework specifies requirements for declarative specification, making the underlay network architecture agnostic for ML applications linked to a specific network function. ML architecture should be able to provide dynamic specification of data sources, ML models, output targets, and constraints.

Finally, all of ML functionalities have to be managed in efficient and seamless manner. Different applications and optimization problem spaces demand different ML models with specific parameters and optimization techniques. Moreover, as previously explained, the framework offers dynamical addition of various data sources. These data sources, in general, are of heterogeneous nature, requiring that the ML model selection for a given application is selected dynamically and adaptively. Consequently, ML functionalities in the network should provide performance monitoring and suitable orchestration based on the output of the models. In addition to optimization and orchestration of VNFs and the underlay network, the output could be compared to given thresholds and reused for model corrections. All of the activities performed in ML functions need to be transparent for the network, meaning that training, updating and scaling of the model must not cause any impact or disturbance to the live network. These requirements are sublimed in the high-level architectural model recommended in ITU-T Y.3172 specification, illustrated in Figure 1.

B. ETSI ENI Framework

Parallel to recommendations presented by ITU, ETSI derived its own recommendation regarding the AI framework, named ENI (Experiential Network Intelligence) [15]. The goal behind the architecture presented is to provide a unified distributed platform, capable of addressing problems of the next generation networks using AI. The basis is a policy-driven closed loop model, which can dynamically adapt the network behavior in accordance with change of inputs. The system utilizing services offered by the ENI system is denoted as “Assisted System” (AS). While ITU architecture seems more modular, in terms of ML functionality placement, the ETSI architecture describes the ENI system as isolated segment/box with API interface for communication with the Assisted System (Figure 2).

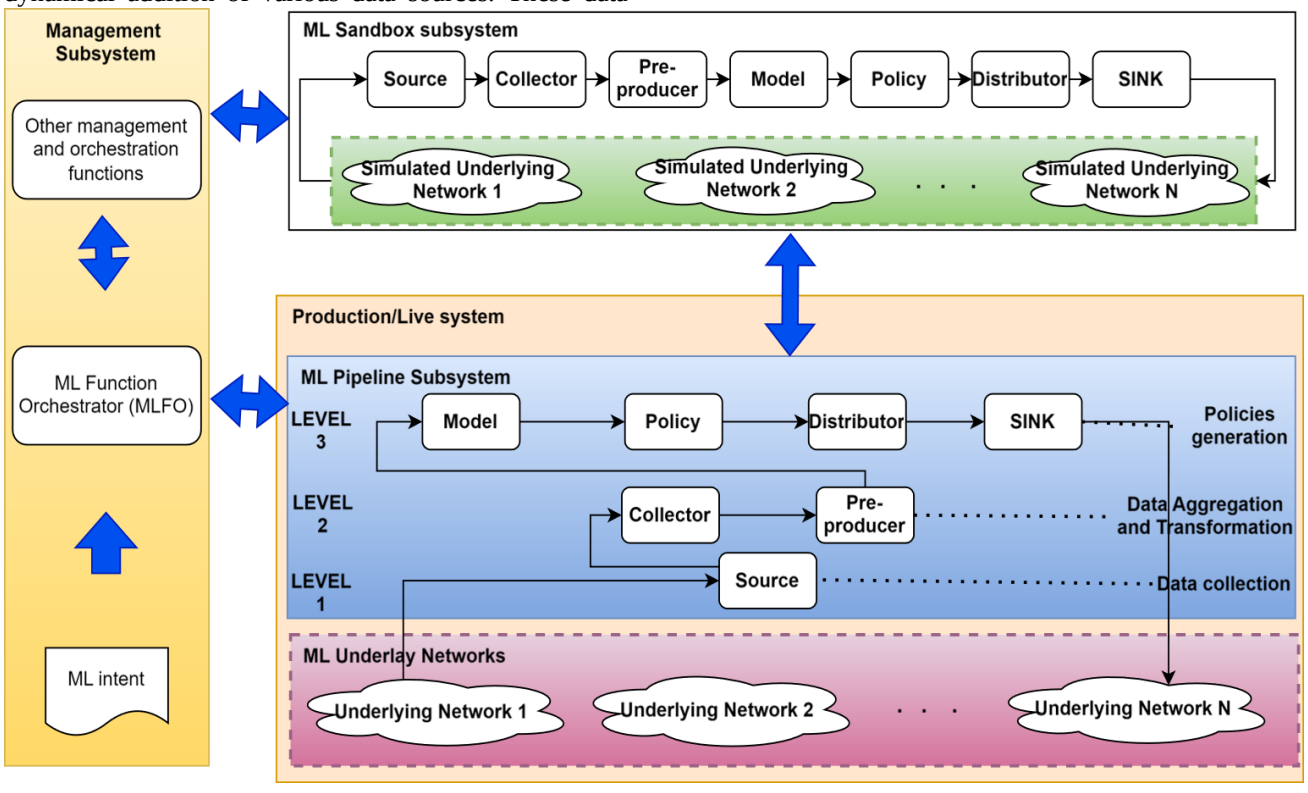

Fig. 1 ITU-T.3172 AI/ML Architecture Framework

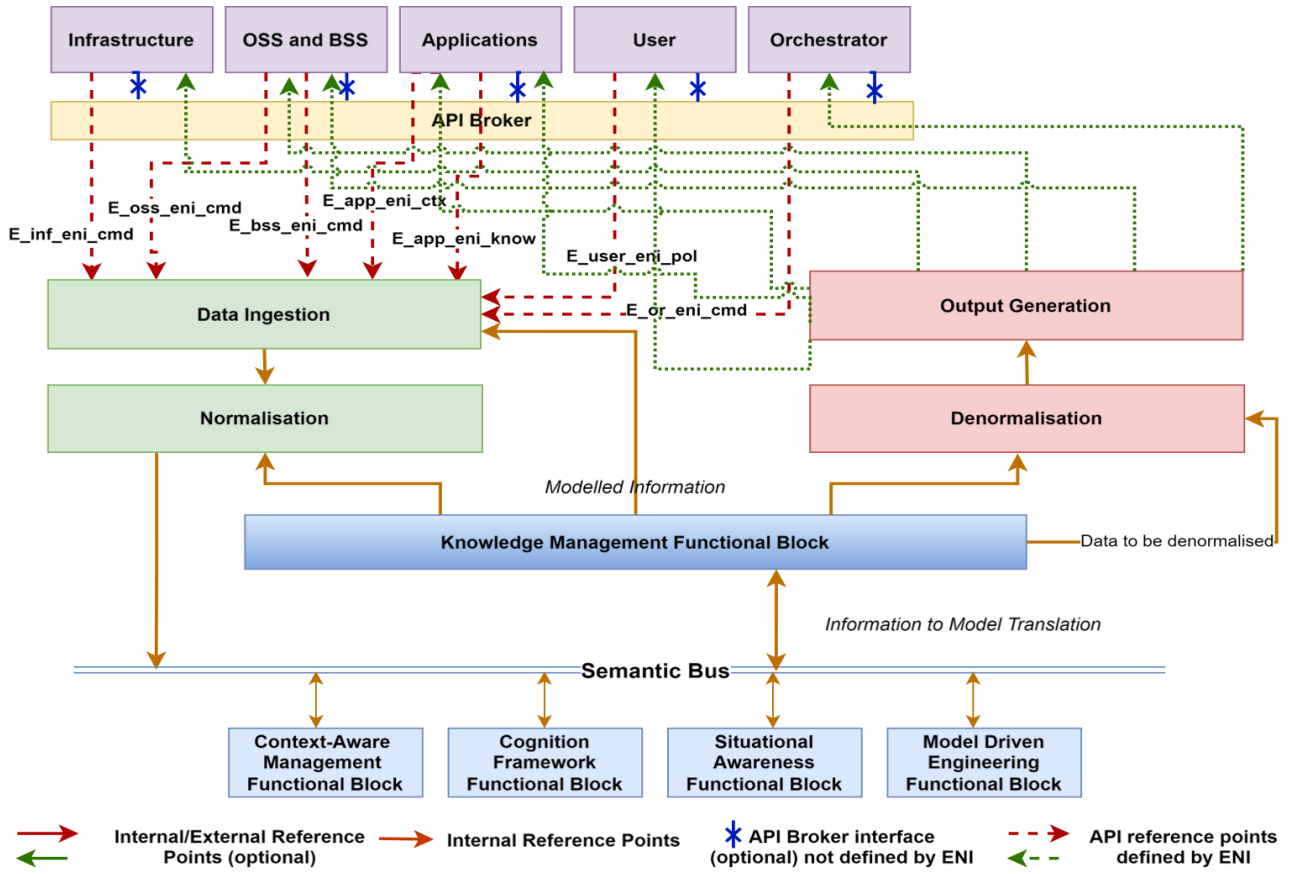

Fig. 2 ENI System architecture with defined interfaces and reference points

A major part is devoted to the API Broker, which is crucial for communication with assisted systems that does not support ENI External Reference Points (RESTful interfaces) and ENI APIs. Since AI presents a new level of functionality in the networks, it is logical to assume that NFs interfaces are not directly compatible with the aforementioned. The recommendation classifies the AS in three levels, based on AI capabilities – none, only for non-real-time decisions, and real and non-real time capable AI AS systems. The ENI system presents two modes of operation, i.e. "recommendation mode" and "management mode". The first is used only for providing recommendations to the AS, which can later be used in the internal (AS) deduction of policies and rules. The second is used for providing decisions and commands to the Assisted System. Furthermore, a hybrid mode is presented where, after the AS validates that recommendations provided in "recommendation mode" are compliant with the internally derived results, it can switch to "management mode". The ENI system is divided in three logical functional blocks: input processing, analysis, and output generation. The input generation is consisted of two sub-blocks: data ingestion and normalization functional blocks. As the name suggest, the purpose of data ingestion is to collect data from various sources and additionally apply common data processing techniques to enable further processing by other ENI functional blocks. As previously defined in ITU architecture, data streams can be ingested by different network domains (Access Network, Transport, and Core) or Assisted Systems (separate segments in the network domains). The communication is performed by using External Reference Points or API Broker. This stage can be mapped to data preprocessing in classical ML, with stages as data filtering, data correlation, data augmentation, and data labeling. In addition, if private or biometric data is used, ENI suggests a data anonymization and pseudonymization phase. The normalization functional block serves as mediator between the external systems and the ENI system, i.e. it unifies data parameters towards internal ENI functional blocks. The generalization enables vendor interoperability and neutrality. Next in line is the analysis phase. It consists of knowledge management, context awareness, cognition management, situation awareness, model-driven engineering, and policy management functional block. The knowledge management block serves for differentiation between known facts, axioms and inference. It uses different mathematical models for presenting information and entropy. This block is the heart of the ENI system and is used by every other functional block.

Context Awareness Management Function serves for extracting the state and environment from which rules can be derived for a given subset of entities in the Assisted System.

The brain of the ENI system is the cognition management functional block. It evaluates the meaning of processed data, considering both the context and predefined objectives of the system of interest.

The situational awareness block provides real-time monitoring and understanding of the surrounding environment, enabling informed decision-making. Meanwhile, the model-driven function block utilizes predefined models to guide its actions and responses, ensuring efficient and effective system operation.

The last layer is output generation. It consists of two blocks: denormalization and output generation functional blocks. Denormalization is used for translating ENI system information and data from various internal formats into standardized form. For example, customer data can be saved in different formats as Lightweight Directory Access Protocol (LDAP) and Relational Database Management System (RDBMS). The output generation functional block can be integrated or separated from the denormalization block. It converts data received from the denormalization step (recommendations or management configurations) into format suitable for the Assisted System of interest. The overall ENI system architecture is depicted in Figure 2.

C. Fault and Recovery Model

One of the most accentuated features in terms of operations, maintenance and regulatory legislation is the fault and recovery function, presenting an obligatory part of every AI system. ITU described such model in the recommendation ITU-T Y.3177 (Fig.3), which is compliant and follows the basic framework introduced in ITU-T Y.3172. The fundamental components outlined in the model largely adhere to the recommendations outlined in the ENI architecture. The main constituents of the model are resource management and fault management pipelines [10]. The sandbox is a crucial part of the framework, used for simulating scenarios and improving the ML model. This component is particularly vital for fault management as the anticipated number of faults at the production level is minimal, rendering it unsuitable for ML training and refinement. The resource management segment consists of two main components: resource prediction and resource adaptation. The first is used for data gathering (performance metrics, load, and resource utilization) and AI/ML prediction. The inference obtained as output of AI/ML models is further used as basis for resource prediction, subsequently guiding resource allocation and adaptation procedures. The latter is presented by multistage pipeline of decision functions, with tendency for optimal resource slicing. Resource adaptation can be carried in two ways: reactively and proactively. It is defined by three functions: resource arbitration, network function migration, and network slice reconfiguration. The main aim of the resource arbitration function is to optimally allocate available resources of the underlying network across different network slices, taking into consideration the plethora of parameters that describe the requirements and importance of services (QoS, delay, jitter, bandwidth, etc.). AI/ML models are crucial for executing optimization procedures of this caliber. Network function migration functionality is responsible for agile and effective migration of vNFs/cNFs, aiming at meeting the service requirements while optimizing the overall performance of the network. It delegates the process of vNFs/cNFs placement and resource utilization of different physical nodes in the underlay infrastructure.

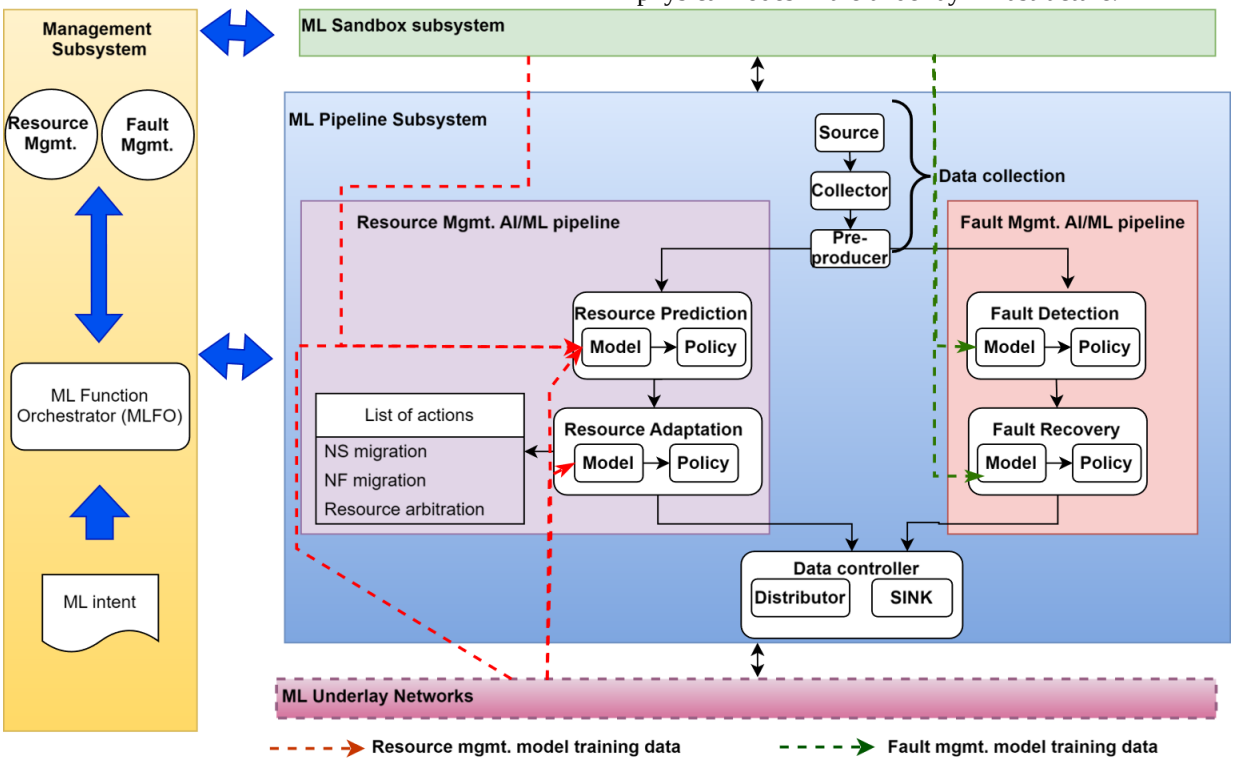

Fig. 3 ITU-T Y.3177 Framework Recommendation for Resource and Fault Management

However, this function cannot instantiate additional physical resources, i.e. can only manipulate with the ones linked to the network slices of interest. To make the model more flexible, network slice reconfiguration is introduced. This function operates slower than the previous two, because it requires interactions with underlay resource

controllers. The network slice reconfiguration enables scale in/out of new physical nodes, supporting specific NFs.

Fault management is one of the most important segments of implementing different security mechanisms in the AI/ML network model. It consists of fault detection and fault recovery. Verification and improvement of different AI/ML models is generally performed by using the AI/ML sandbox.

I. III. STANDARDIZATION AND REGULATION

With the growing popularity of AI, regulatory bodies worldwide are focusing on standardizing and regulating its use. In April 2021, the European Commission proposed the first European AI regulatory framework. Over the next two years, various groups worked on defining AI use, its weaknesses, and security flaws. In December 2023, an agreement was reached with the European Parliament, leading to the final adoption of the EU AI Act on March 13, 2024, with 523 votes in favor, 46 against, and 49 abstentions [18]. The Act classifies AI use into four categories: unacceptable (banned), high risk, limited risk, and minimal risk. It also covers general-purpose AI models used by major tech companies. Non-compliance with banned AI practices can result in fines up to EUR35 mil. or 7% of a company's global annual turnover, whichever is higher [19].

In the United States., AI regulation is largely state-level, with no comprehensive federal framework. Between 2016 and 2022, 14 states have passed AI-related legislation, with Maryland being the leader. However, only 9 out of 88 federal AI legislative acts were passed [20]. In October 2023, President Joe Biden issued an executive order (EO) on “Safe, Secure, and Trustworthy Development and Use of AI” [21]. This move suggests that the U.S. telecommunications sector may face similar regulations to the EU AI Act [22].

China's AI legislation is divided into two segments: government AI systems and the private sector [23]. The government sector faces looser regulations, with most categories permitted, including social scoring, already implemented in some areas. China has stricter laws for “algorithmic recommendation” due to the backlash against *ByteDance*'s media apps in 2017. In 2021, China introduced legislation requiring algorithm providers to uphold societal values and comply with standards similar to the GDPR. Recommendations must align with ethical principles and avoid promoting addictive content. All recommendation algorithms must be submitted for government approval.

On July 13, 2023, China introduced the “Interim Measures for Management of Generative Artificial Intelligence Services”, in effect from August 15, 2023 [24]. These regulations are vital for AI models like chatbots and AI agents in telecommunications and personalized content delivery.

Although AI regulations in telecommunications will likely be similar, this paper adheres to the EU AI Act. Given the definition of high-risk AI systems, many telecommunications use cases will fall under this category. High-risk AI includes non-banned biometrics, critical infrastructure (e.g., digital infrastructure, road traffic, utilities), education, law enforcement, and administration of justice and democratic processes. Telecommunications, as part of the critical infrastructure, are subject to these regulations. Key use cases involve data processing for network management, personalized content, targeting, trend analysis, and churn analysis. Profiling, a key business driver, is considered high-risk under Article III of the EU AI Act and aligned with GDPR definitions [19].

Telecommunications network equipment, categorized as critical infrastructure [Annex I, point (6)], relies on software packages on COTS hardware with APIs (HTTP/REST) between network functions. Annex IV mandates detailed documentation for software and APIs related to ML functionalities. To ensure compliance with the legislation, high-risk systems must adhere to requirements and provide appropriate documentation. AI system providers must ensure their products comply with the EU harmonization legislation [Annex I, Section A]. The Act mandates a continuous risk management system, supported by documentation as specified in Article 11, for testing high-risk systems against predefined thresholds and metrics.

While some network functions (RAN, CN, MEC) can operate without personal data, many business use cases involve processing biometric and personal data. Access to customer data (e.g., CRM, CDR/EDR, DPI systems, chatbots) must comply with GDPR Article 9(1) and national laws, unless prohibited by the EU Act. The risk management system must address risks of biased or discriminatory results based on biometric data such as social status, race, or ethnicity. Data management must align with GDPR, which requires a legitimate basis for data processing, such as consent or contractual agreement.

Chatbots, often general-purpose AI systems (GPAIS), must follow special design criteria laid out in Annex XI and Annex XIII. In addition to internal controls, ML providers are subject to external regulatory oversight. Article 12 mandates automatic log keeping for high-risk AI systems throughout their lifetime, with retention of at least six months (Article 19). High-risk AI systems also require certification, with a validity period of four years (Annex III).

In addition to formal legislation, numerous ethical playbooks and recommendations from organizations like GSMA provide methodologies and self-assessment tools for implementing lawful AI/ML practices in telecom networks. GSMA’s AI for Impact (AI4I) initiative outlines three levels of responsibility for ethical AI deployment. The first level involves AI product managers and teams who manage low-risk AI applications using self-assessment tools. The second level, ethics committee, evaluates higher-risk applications with expert input. The executive board, at the third level, makes final deployment decisions, often in consultation with the ethics committee. Many CSPs have established internal bodies for AI/ML risk and security assessments, both pre-deployment and during the system's lifecycle.

Orange formed its Data and AI Ethics Council in March

2021, consisting of 11 independent experts from diverse professional backgrounds. This independent body advises on ethical issues and appoints Data and AI Ethics Officer in each country for local assessment and reporting to the Council. Similarly, *Telstra* created a Risk Council for AI and Data (RCAID), which evaluates AI/ML software at all stages of deployment. For high-risk applications, the evaluation is escalated to *Telstra*'s Data and AI Council. *Telefonica* follows the Responsible AI by Design methodology, which incorporates a three-tiered structure to assess AI/ML risk levels.

These regulations aim to shape AI use cases and business models while ensuring fair market competition and interoperability between ML functions and network interfaces [26].

II. IV. Business: Aims, Opportunities and Realizations

The main drivers of commercially available technologies are business use cases and opportunities. Emergence of AI/ML models has created new business models, profit avenues, and savings. Many companies have started implementing these models across various segments of their networks and business portfolios, aligning with forecasted growth. Numerous papers and reports highlight potential use cases. The Body of European Regulators for Electronic Communications (BEREC) classifies AI use cases into six main areas: network and capacity planning, channel modeling, dynamic spectrum sharing (DSS), QoS optimization, security optimization, and fraud detection [27].

In the RAN segment, *Nokia* and *NVIDIA* announced a collaboration to combine Nokia Cloud RAN with NVIDIA's AI-powered processing [28]. This may enhance the benefits of Nokia Cloud RAN, including a 15% reduction in base station power consumption, 70% fewer alarms, and 80% efficiency gains with zero-touch optimization. Additionally, Open Radio Access Networks (O-RAN) promote open standards, enabling cost-efficiency and flexibility in telecom networks. AI/ML integration in O-RAN supports real-time network optimization, intelligent resource management, and automation. Companies like *Nokia* and *NVIDIA* are integrating AI-driven O-RAN solutions for improved service delivery and scalability [27] [28].

Intelligence and automation are crucial across all telecom networks, with the ultimate goal being end-to-end service optimization for guaranteed QoS. This is known as zero-touch operation. ETSI formed the Zero-Touch Network and Service Management (ZSM) group in 2017 to create a framework for interoperability among vendor-specific solutions [29] [30]. *Nokia* has reported an 80% operational efficiency increase in a proof-of-concept with a North American operator using their Self-Organizing Network (SON) software, which utilizes AI/ML for cognitive automation. *SK Telecom*'s TANGO (Telco Advanced Next-Generation OSS) is another successful implementation, offering an AI-assisted network operating system that integrates and analyzes data from various network segments [31]. TANGO is expected to recoup CAPEX and OPEX within five years and further reduce costs by 40% over the next five years. The zero-touch provisioning market was valued at USD2,772.13 mil.in 2022 and is forecasted to grow to USD7,544.15 mil.by 2032, with CAGR of 10.6% [32].

NTT, *Huawei* and other industry leaders are advancing development of versatile language models, targeting a wide range of applications across different sectors. These models, similar to ChatGPT, offer natural language understanding and generation across sectors [33]. The model comes in two versions: an ultra-lightweight version (600 million parameters) and a lightweight version (7 billion parameters), far smaller than OpenAI's GPT-3 (175 billion parameters). This reduced complexity allows efficient deployment on single GPU or even CPU, lowering training and maintenance costs and providing faster ROI. For context, GPT-3's training requires 1300 MWh, equivalent to one hour of nuclear power generation. NTT's "tsuzumi" model outperforms GPT-3.5, scoring 81.3% on the Rakuda benchmark. Its ability to adapt to different business models makes it suitable for customer care operations in telecoms.

Huawei has developed telecommunications-specific models, NET4AI and AI4Net, which cater to the new generation of networks. NET4AI supports AI-as-a-service (AIaaS), forming the backbone for AI-powered services, while AI4Net focuses on intelligent operations, enhancing network performance, resource management, security, and user experience [34].

In addition to backend applications, several use cases directly engage end consumers. For instance, *AT&T* enhanced its "Call Before You Dig" platform with AI/ML, improving geospatial recognition and report analysis. This led to a 7% reduction in miles traveled per dispatch and 5% increase in productivity [35]. *Deutsche Telekom* deployed three chatbots: Tinka, Vanda, and Hub:raum. Tinka, used in Austria, answers 80% of customer queries, forwarding the rest for human analysis. Vanda is a similar NLP-based chatbot, and Hub:raum assists with recruitment queries [36].

Vodafone introduced its chatbot, TOBi, which enhances customer communication through mobile apps, WhatsApp, and SMS, automating two-thirds of customer interactions in Italy, leading to a 68% improvement in customer experience [37]. *Colt Technology Services* launched the Sentio AI/ML assistant, automating service provisioning and providing flexible bandwidth in real time.

Aggressive adoption of AI/ML in telecom networks drives technological advancement, reduces CAPEX/OPEX, and increases revenues. The AI telecom market was valued at USD1.45 billion in 2022, with forecasted CAGR of 28.2% from 2023 to 2030. North America accounted for 34.8% of the market in 2022, but Asia Pacific is expected to have the fastest growth due to investments in China and India [38]. China leads AI patents with 61.1%, while the U.S. invest USD67.2 billion in the private AI sector, about 8.7 times more than China [39]. McKinsey reports that 42% of companies reduce costs with AI, and 59% see revenue increases, with tech, media, and telecom sectors leading AI adoption for product and

service development [40]. AI-driven predictive maintenance can cut telecom maintenance costs by 30-40%, and behavior prediction models may reduce churn by 10-15%. Over 75% of telecom companies plan to invest in AI systems in the next three years [41].

III. V. CONCLUSION

This paper explores AI/ML advancements and challenges in the telecom sector. A robust technological and regulatory framework is essential for ensuring interoperability, privacy, safety, and business sustainability. Key recommendations from ITU-T (Recommendation Y.3172) and ETSI (ENI framework) serve as the foundation, with fault and recovery functionalities crucial for model sustainability. Regulatory developments, including the EU AI Act, the U.S. state-level legislation, and China's dual-focused framework, emphasize the need for ethical AI deployment. Industry-led initiatives like GSMA's Ethical Requirements playbook further support responsible AI use. Legislative frameworks will shape telecom network development, especially for high-risk applications, though diverse global regulations complicate deployments. AI/ML integration unlocks new business opportunities, particularly in network optimization and customer service. AI-powered chatbots by *AT&T*, *Deutsche Telekom*, and *Vodafone* have improved customer experience with faster query resolution and accessibility. Statistical trends indicate AI's transformative impact on telecom operations, maintenance, and architecture.

REFERENCES

[1] Toni Janevski. "QoS for Fixed and Mobile Ultra-Broadband". Wiley – IEEE Press, 2019

[2] Toni Janevski. "Future Fixed and Mobile Broadband Internet, Clouds, and IoT/AI". Wiley – IEEE Press, 2024.

[3] Huawei. "6G: The Next Horizon. From Connected People and Things to Connected Intelligence", 2020.

[4] Nokia. "Responsible AI for Telecom", 2021.

[5] NVIDIA. "State of AI in Telecommunications: 2024 Trends Survey Report", https://resources.nvidia.com/en-us-ai-in-telco/state-of-ai-in-telco-2024-report [last retrieved in October 2024].

[6] Recommendation ITU-T Y.3115, "AI-enabled cross-domain network architectural requirements and framework for future networks including IMT-2020". 2022.

[7] Recommendation ITU-T Y.3170, "Requirements for machine learning-based quality of service assurance for the IMT-2020 network". 2018.

[8] Recommendation ITU-T Y.3172, "Architectural framework for machine learning in future networks including IMT-2020". 2019.

[9] Recommendation ITU-T Y.3183, "Framework for network slicing management assisted by machine learning leveraging quality of experience feedback from verticals". 2023.

[10] Recommendation ITU-T Y.3177, "Architectural framework for artificial intelligence-based network automation for resource and fault management in future networks including IMT-2020". 2021.

[11] ETSI. ETSI GS ENI 001 V3.2.1, "Experiential Networked Intelligence (ENI); ENI Use Cases". May 2023.

[12] ETSI. ETSI GS ENI 002 V3.2.1, "Experiential Networked Intelligence (ENI); ENI Requirements". April 2023.

[13] ETSI. ETSI GR ENI 003 V1.1.1, "Experiential Networked Intelligence (ENI); Context-Aware Policy Management Gap Analysis". May 2018.

[14] ETSI. ETSI GR ENI 004 V3.1.1, "Experiential Networked Intelligence (ENI); Terminology". July 2023.

[15] ETSI. ETSI GS ENI 005 V3.1.1, "Experiential Networked Intelligence (ENI); System Architecture". June 2023

[16] ETSI. ETSI GS ENI 006 V2.1.1, "Experiential Networked Intelligence (ENI); Proof of Concepts Framework". May 2020.

[17] ETSI. Ongoing PoCs, https://eniwiki.etsi.org/index.php?title=Ongoing_PoCs, [last retrieved in October 2024] .

[18] European Parliament. "Artificial Intelligence Act: MEPs Adopt Landmark Law". 2024.

[19] European Parliament. "Artificial Intelligence Act". 2024.

[20] HAI. "AI Index Report 2023". 2023.

[21] White House. FACT SHEET: President Biden Issues Executive Order on Safe, Secure, and Trustworthy Artificial Intelligence, (2023-10), https://www.whitehouse.gov/briefing-room/statements-releases/2023/10/30/fact-sheet-president-biden-issues-executive-order-on-safe-secure-and-trustworthy-artificial-intelligence/, [last retrieved in October 2024].

[22] European Parliament. "United States' Approach to Artificial Intelligence" 2024.

[23] Matt Sheehan/ "China's AI Regulations and How They Get Made". Carnegie Endowment for International Peace, Washington, DC, 2023.

[24] China Law Translate. "Interim Measures for Management of Generative Artificial Intelligence Services". July 13, 2023,

[25] Official Journal of the European Union, REGULATION (EU) 2016/679 OF THE EUROPEAN PARLIAMENT AND OF THE COUNCIL, April 27, 2016.

[26] GSMA. "The AI Ethics Playbook: Implementing Ethical Principles into Everyday Business". 2022.

[27] BEREC. "Report on the impact of Artificial Intelligence (AI) solutions in the telecommunications sector on regulation". June 8, 2023.

[28] Nokia. "Nokia to Revolutionize Mobile Networks with Cloud RAN and AI Powered by NVIDIA". February 24, 2024.

[29] ETSI. "Zero-touch Network and Service Management". December 7, 2017.

[30] ETSI. "Zero-touch network Service Management group renewed for two years". October 5, 2023.

[31] GSMA. "Innovator Profile: SKT Tango". October 14, 2019.

[32] POLARIS. "AI in Telecommunication Market Share, Size, Trends, Industry Analysis Report, By Region, And Segment Forecasts, 2023 – 2032". January 2024.

[33] NTT R&D. NTT's Large Language Models 'tsuzumi'. April 25, 2024, https://www.rd.ntt/e/research/LLM_tsuzumi.html, [last retrieved in October 2024].

[34] HuaweiTech, NET4AI: Supporting AI as a Service in 6G, November, 2022, https://www.huawei.com/en/huaweitech/future-technologies/net4ai-supporting-ai-as-a-sevice-6g, [last retrieved in October 2024].

[35] Eric Zavesky. "Call Before You Dig: Using AI and Data Science to Protect Buried Cables and Keep Construction Projects on Track". December 1, 2023, https://about.att.com/blogs/2023/call-before-you-dig.html, [last retrieved in October 2024].

[36] AIT Staff Writer. "Top 10 AI-Powered Telecom Companies in World", AITHORITY. March 4, 2020, https://aithority.com/technology/analytics/top-10-ai-powered-telecom-companies-in-world, [last retrieved in October 2024].

[37] Neil Blafden. "Artificial brains and predictive care: Vodafone's digital journey". Vodafone. December 15, 2019, https://www.vodafone.co.uk/newscentre/viewpoint/artificial-brains-and-predictive-care-vodafones-digital-journey/, [last retrieved in October 2024].

[38] GVR. "AI in Telecommunication Market Size, Share & Trends Analysis Report By Application (Network Security, Network Optimization, Customer Analytics, Virtual Assistance, Self-Diagnostics), By Region, And Segment Forecasts, 2023 – 2030", https://www.grandviewresearch.com/industry-analysis/artificial-intelligence-telecommunication-market#, [last retrieved in October 2024].

[39] HAI. "AI Index Report 2024", 2024. https://aiindex.stanford.edu/wp-content/uploads/2024/04/HAI_AI-Index-Report-2024.pdf, [last retrieved in October 2024].

[40] McKinsey. "The State of AI in 2023: Generative AI's Breakout Year". August, 2023.

[41] GITNUX. "MARKETDATA REPORT 2024: AI in the Telecommunications Industry Statistics". April 2024.

Journal of Electrical Engineering and Information Technologies, Vol. **9,** No.1, pp. 116–119 (2024)
In print: ISSN 2545–4250
On line: ISSN 2545–4269

INSTRUCTIONS FOR AUTHORS

The *Journal of Electrical Engeneering and Information Technologies* is published twice yearly. The journal publishes **original scientific papers, short communications, reviews** and **professional papers** from all fields of electrical engineering.

The journal also publishes (continuously or occasionally) the bibliographies of the members of the Faculty, book reviews, reports on meetings, informations of future meetings, important events and data, and various rubrics which contribute to the development of the corresponding scientific field.

Original scientific papers should contain hitherto unpublished results of completed original scientific research. The number of pages (including tables and figures) should not exceed 15 (28 000 characters).

Short communications should also contain completed but briefly presented results of original scientific research. The number of pages should not exceed 5 (10 000 characters) including tables and figures.

Reviews are submitted at the invitation of the Editorial Board. They should be surveys of the investigations and knowledge of several authors in a given research area. The competency of the authors should be assured by their own published results.

Professional papers report on useful practical results that are not original but help the results of the original scientific research to be adopted into scientific and production use. The number of pages (including tables and figures) should not exceed 10 (18 000 characters).

Acceptance for publication in the Journal obliges the authors not to publish the same results elsewhere.

SUBMISSION

The article and annexes should be written on A4 paper with margins of 2.5 cm on each side with a standard font Times New Roman 11 points and should be named with the surname of the first author and then if more and numbered. It is strongly recommended that on MS Word 2003 or MS Word 2007 and on PDF files of the manuscript be sent by e-mail:

JEEIT@feit.ukim.edu.mk.

A letter must accompany all submissions, clearly indicating the following: title, author(s), corresponding author's name, address and e-mail addres(es), suggested category of the manuscript and a suggestion of five referees (their names, e-mail and affiliation).

Articles received by the Editorial Board are sent to two referees (one in the case of professional papers). The suggestions of the referees and Editorial Board are sent to the author(s) for further action. The corrected text should be returned to the Editorial Board as soon as possible but in not more than 30 days.

PREPARATION OF MANUSCRIPT

The papers should be written in the shortest possible way and without unnecessary repetition.

The original scientific papers, short communications and reviews should be written in English, while the professional papers may also be submitted in Macedonian.

Only SI (Système Internationale d'Unites) quantities and units are to be used.

Double subscripts and superscripts should be avoided whenever possible. Thus it is better to write $\nu_3(PO_4)$ than $\nu_{3_{PO_4}}$ or exp(–E/RT) than $e^{-E/RT}$. Strokes (/) should not be used instead of parentheses.

When a large number of compound have been analyzed, the results should be given in tabular form.

Manuscript should containt: title, author(s) full-name(s), surname(s), address(es) and e-mail of the corresponding author, short abstract, key words, introduction, experimental or theoretical back-ground, results and discussion, acknowledgment (if desired) and references.

The **title** should correspond to the contents of the manuscript. It should be brief and informative and include the majority of the key words.

Each paper should contain an **abstract** that should not exceed 150 words and **3–5 key words**. The abstract should include the purpose of the research, the most important results and conclusions.

The **title**, **abstract** and **key words** should be translated in Macedonian language. The ones written by foreign authors will be translate by the Editorial Board.

In the **introduction** only the most important previous results related to the problem in hand should be briefly reviewed and the aim and importance of the research should be stated.

The **experimental** section should be written as a separate section and should contain a description of the materials used and methods employed – in form which makes the results reproducible, but without detailed description of already known methods.

Manuscripts that are related to **theoretical studies**, instead of experimental material, should contain a sub-heading and the **theoretical background** where the necessary details for verifying the results obtained should be stated.

The **results** and **discussion** should be given in the same section. The discussion should contain an analysis of the results and the **conclusions** that can be drawn.

Figures (photographs, diagrams and sketches) and **mathematical formulae** should be inserted in the correct place in the manuscript, being horizontally reduced to 8 or 16 cm. The size of the symbols for the physical quantities and units as well as the size of the numbers and letters used in the reduced figures should be comparable with the size of the letters in the main text of the paper. Diagrams and structural formulae should be drawn in such a way (e.g. black Indian ink on white or tracing paper) as to permit high quality reproduction. The use of photographs should be avoided. The tables and the figures should be numbered in Arabic numerals (e.g. Table 1, Figure 1). Tables and figures should be self-contained, i.e. should have captions making them legible without resort to the main text. The presentation of the same results in the form of tables and figures (diagrams) is not permitted.

Figures and tables must be centred in the column. Large figures and tables may span across both columns (Figure 1).

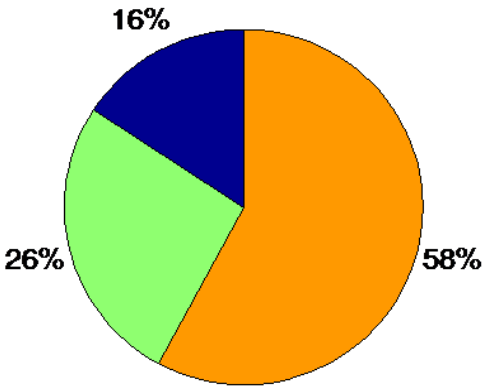

Fig. 1. Example of a graph and a single-line caption (collour)

Graphics may be full colour. Please use only colours which contrast well both on screen and on a black-and-white hardcopy because the Journal is published in black-and-white, as shown in Figure 2. The colour version is only for the electronic version of the Journal.

Please check all figures in your paper both on screen and on a black-and-white hardcopy. When you check your paper on a black-and-white hardcopy, please ensure that:

– the colours used in each figure contrast well,

– the image used in each figure is clear,

– all text labels in each figure are legible.

Please check all figures in your paper both on screen and on a black-and-white hardcopy. When you check your paper on a black-and-white hardcopy, please ensure that the image used in each figure is clear and all text labels in each figure are legible.

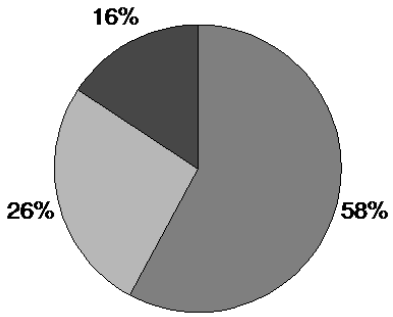

Fig. 2. Example of a graph and a single-line caption (black-and-white)

Fig. 3. Example of an image as it will appear at the electronic version of the Journal and a multi-line caption

Footnotes are also not permitted.

The **reference** should be given in a separate section in the order in which they appear in the text. The surname of one or two authors may be given in the text, whereas in the case of more than two authors they should be quoted as, for example:

Examples of reference items of different categories shown in the References section include:

- example of a book in [1]
- example of a book in a series in [2]
- example of a journal article in [3]
- example of a conference paper in [4]
- example of a patent in [5]
- example of a website in [6]
- example of a web page in [7]
- example of a databook as a manual in [8]
- example of a datasheet in [9]
- example of a master/Ph.D. thesis in [10]
- example of a technical report in [11]
- example of a standard in [12]

All reference items must be in 9 pt font. Please use Regular and Italic styles to distinguish different fields as shown in the References section. Number the reference items consecutively in square brackets (e.g. [1]).

When referring to a reference item, please simply use the reference number, as in [2]. Do not use "Ref. [3]" or "Reference [3]" except at the beginning of a sentence, e.g. "Reference [3] shows …". Multiple references are each numbered with separate brackets (e.g. [2, 3], [4–8]).

The **category** of the paper is proposed by the author(s), but the Editorial Board reserves for itself the right, on the basis of the referees' opinion, to make the final choice.

Proofs are sent to the author(s) to correct printers' errors. Except for this, alterations to the text are not permitted. The proofs should be returned to the Editorial Board in 2 days.

The author(s) will receive, free of charge, 1 reprint of every paper published in the Journal.

REFERENCES

[1] Surname, N(ame).; Surname, N(ame). (Year): *Name of the Book*, Publisher.

[2] Surname, N(ame).: Surname, N(ame). (Year): *Name of the Book*, Name of the Series. Publisher, **vol.** XXX.

[3] Surname, N(ame).; Surname N(ame). (Year): Title of the article, *Name of the Journal*, **Vol. XX,** No. XX, pp. XXX–XXX.

[4] Surname, N(ame).; Surname N(ame). (Year): Title of the article, *Proceedings of the Conference (Name)*, **Vol. XX,** pp. XXX–XXX.

[5] Surname, N(ame).; Surname N(ame). (Date dd. mm. yyyy): *Name of the Patent*, Institution that issued the patent & Number of the patent.

[6] N.N. (Year): *The XXX web site*, web address.

[7] Surname, N. (Year): *XXX homepage on XXX*, web address.

[8] N.N. (Year): *Title of the Manual*, Name of the Organization.

[9] N.N.: *XXX data sheet*, Name of the Organization.

[10] Surname, N. (Year): *Title of the Thesis*, Master/Ph.D. thesis (in Language), Institution.

[11] Surname, N(ame)., Surname, N(ame). (Year): *Title of the Report*, organization that issued the report, Number of the report.

[12] Institution that issued the standard, *Name of the Standard*, & Number of the standard (Year).